© 2022. Published by The Company of Biologists Ltd | Development (2022) 149, dev200115. doi:10.1242/dev.200115

STEM CELLS AND REGENERATION

RESEARCH ARTICLE

RhoA/ROCK signaling antagonizes bovine trophoblast stem cell self-renewal and regulates preimplantation embryo size and differentiation

Viju Vijayan Pillai[1], Tiffany G. Kei[1], Shailesh Gurung[1], Moubani Das[1], Luiz G. B. Siqueira[2,3], Soon Hon Cheong[4], Peter J. Hansen[2] and Vimal Selvaraj[1,*]

ABSTRACT

Exponential proliferation of trophoblast stem cells (TSC) is crucial in Ruminantia to maximize numerical access to caruncles, the restricted uterine sites that permit implantation. When translating systems biology of the undifferentiated bovine trophectoderm, we uncovered that inhibition of RhoA/Rock promoted self-renewing proliferation and substantially increased blastocyst size. Analysis of transcripts suppressed by Rock inhibition revealed transforming growth factor β1 (TGFβ1) as a primary upstream effector. TGFβ1 treatment induced changes consistent with differentiation in bTSCs, a response that could be replicated by induced expression of the bovine ROCK2 transgene. Rocki could partially antagonize TGFβ1 effects, and TGFβ receptor inhibition promoted proliferation identical to Rocki, indicating an all-encompassing upstream regulation. Morphological differentiation included formation of binucleate cells and infrequent multinucleate syncytia, features we also localize in the *in vivo* bovine placenta. Collectively, we demonstrate a central role for TGFβ1, RhoA and Rock in inducing bTSC differentiation, attenuation of which is sufficient to sustain self-renewal and proliferation linked to blastocyst size and preimplantation development. Unraveling these mechanisms augments evolutionary/comparative physiology of the trophoblast cell lineage and placental development in eutherians.

KEY WORDS: Trophoblast, Blastocyst, Stem cells, Implantation, Placenta, Pregnancy

INTRODUCTION

The fundamental morphology of embryonic development leading to formation of the blastocyst is highly conserved among eutherian mammals. During this time, the trophectoderm functions to support blastocoel formation (Aziz and Alexandre, 1991; Kawagishi et al., 2004; Watson and Barcroft, 2001; Wiley, 1984), promoting both a microenvironment to sustain development in the inner cell mass, and separation of extra-embryonic development. Subsequent phases of trophectoderm functional differentiation include species-specific adaptations that effect signaling for maternal recognition of pregnancy, morphological and functional preparation for implantation, and establishment of a pertinent placenta. Most of what we know regarding trophoblast cell biology is from studies conducted in human and rodent systems, both of which establish a hemochorial interface in placental classification (Grosser, 1927; Mossman, 1937). In these species, maternal recognition of pregnancy is mediated by trophoblast secretion of chorionic gonadotropin (Finkel, 1931; Gey et al., 1938; Zondek, 1930; Zondek and Aschheim, 1927), which supports luteinization that sustains ovarian progesterone production (Hirose, 1920), and implantation involves trophoblast invasion into the uterine stroma, which establishes a direct vascular association with maternal blood (Soares et al., 2018). Although placentae across different clades can be considered homologous, fundamental morphological and functional cellular distinctions are apparent in both the physical enveloping of the growing fetus and the adoption of optimal apposition between fetal and maternal circulatory systems (Bazer et al., 1991; Carter, 2012; Roberts et al., 2016).

The epitheliochorial placental interface seen in sub-order Ruminantia emerged later in evolution by divergence from endothelial-hemochorial forms (Wildman et al., 2006). In this interface, apical membranes of the maternal uterine epithelium and the fetal chorion are interdigitated, with no loss of structural components that separate maternal and fetal blood (Mossman, 1937; Wathes and Wooding, 1980). Most distinctive for bovids is that maternal-fetal appositions are restricted to multiple macromorphologically distinct regions, termed caruncles, across the uterine endometrium (Atkinson et al., 1984; Yamauchi, 1964). Countering this anatomical spread of caruncles, preimplantation development after blastocyst entry into the uterus involves dramatic proliferation of undifferentiated trophectodermal cells driving embryo elongation to occupy almost the entire length of both uterine horns without any attachments (Chang, 1952). This tremendous proliferation rate during which an ‘ovoid’ embryo (~2.4×1.2 mm; day 12-13 after ovulation) elongates to a ‘filamentous’ embryo (~160×1.5 mm; day 17-18 after ovulation), which is a ~70-fold increase in trophoblast surface area in 4-5 days (Chang, 1952), ensures extensive trophoblast access to maternal caruncles before initiation of differentiation and implantation (~day 30) (Kingman, 1948; Melton et al., 1951). Proliferation of undifferentiated polygonal ‘stem cells’ as a unicellular layer, and structural changes associated with differentiation that include stratification have been documented in several early studies (Chang, 1952; Greenstein et al., 1958; Wimsatt, 1951). The appearance of a minor subset of larger diplokaryotes/binucleate trophoblast cells (BNCs), together with columnar trophoblast cells, is apparent with differentiation (Greenstein et al., 1958; Wooding, 1992). Another distinctive functional divergence in Ruminantia is that maternal recognition of pregnancy is understood to be informed by interferon τ

[1]Department of Animal Science, College of Agriculture and Life Sciences, Cornell University, Ithaca, NY 14853, USA. [2]Department of Animal Sciences, University of Florida, Gainesville, FL 32611, USA. [3]Embrapa Gado de Leite, Juiz de Fora, MG 36038-330, Brazil. [4]Department of Clinical Sciences, College of Veterinary Medicine, Cornell University, Ithaca, NY 14853, USA.

*Author for correspondence (vs88@cornell.edu)

P.J.H., 0000-0003-3061-9333; V.S., 0000-0002-8728-3765

Handling Editor: Patrick Tam
Received 16 August 2021; Accepted 1 March 2022

Development (2022) 149, dev200115. doi:10.1242/dev.200115

production by the trophectoderm, which is triggered during embryo elongation (Bazer and Thatcher, 2017; Godkin et al., 1984; Imakawa et al., 1987; Roberts et al., 1992). Notwithstanding decades of study on the bovine embryo, mechanisms that control proliferation of the trophectoderm and regulate differentiation remain unknown.

Recently, we described the physiological profile of undifferentiated bovine blastocyst-derived trophoblasts/trophoblast stem cells (TSCs), highlighting the hallmarks of a self-renewing primordial state (Pillai et al., 2019a). In this study, through systematic evaluation of the proteome and transcriptome of bovine TSCs, we identify the core mechanism that sustains stemness and the pathway that induces functional and morphological differentiation. Our findings demonstrate that TGFβ1, RhoA and Rock signaling directs differentiation in bovine trophoblast stem cells, and inhibition of this stimulus/mechanism allows for rapid proliferation via self-renewal, as observed in the trophectoderm during preimplantation embryo elongation.

RESULTS

Rho GTPase signaling is predominant in bovine TSCs

Of the eight dominant pathways enriched in TSC proteomics and TSC transcriptomics datasets [probing our previously generated dataset that defined the identity of the undifferentiated bovine TSC (bTSC) lineage (Pillai et al., 2019a)], we identified that five were common to both, indicating strong correlation between proteome and transcriptome bioinformatic predictions (Table 1). From these two complementary systems biology approaches, Rho GTPase signaling was singled out as predominant in bTSCs, and selected for functional examination.

Inhibition of Rho GTPase signaling enhances proliferation

From the transcriptome, we identified that TSCs express high levels of RhoA, but also express other Rho GTPases (Fig. 1A). To investigate its functional impact, we first inhibited Rho activity using C3, a toxin derived from *Clostridium botulinum* that selectively ADP-ribosylates RhoA, RhoB and RhoC, with RhoA being the preferred substrate (Sekine et al., 1989). In bTSC outgrowths treated with C3, there was an acute increase in the rate of colony growth/proliferation (Fig. 1B). Forced expression of a dominant-negative form of RhoA (DN-RhoA) in these outgrowths also significantly increased proliferation (Fig. 1C). The doxycycline-inducible lentiviral GFP-tagged RhoA T19N mutant expression demonstrated an increased extent of EdU labeling over time in these cells (Fig. 1D), confirming that the change in colony sizes was due to an increase in cell number and not merely a morphological event of colony expansion. This finding also demonstrated that the effect observed with C3 is reproducible by blocking RhoA signaling alone. We then used the inhibitor Y-27632/Rocki (Ishizaki et al., 2000) to investigate the role of Rho-associated coiled-coil forming serine/threonine kinase (Rock), an established target of RhoA; only one isoform, Rock2, was highly expressed in bTSCs (Fig. 1A). Treatment with Rocki reproduced the effect on proliferation seen with C3 and DN-RhoA (Fig. 1E,F).

Table 1. Over-represented pathways identified in TSCs

	Genes	*P* value
Proteome		
Cytoskeletal regulation by Rho GTPase	41	9.36E-20
Chemokine and cytokine signaling	34	2.44E-04
Integrin signaling	29	6.09E-05
Nicotinic acetylcholine receptor signaling	23	2.10E-06
Ubiquitin proteasome	17	1.11E-04
Glycolysis	15	2.13E-08
Dopamine receptor-mediated signaling	13	3.72E-03
Fructose galactose metabolism	8	2.87E-05
TCA cycle	5	1.87E-02
Transcriptome		
Cytoskeletal regulation by Rho GTPase	40	1.97E-04
CCKR signaling	40	9.75E-04
EGF receptor signaling	29	3.38E-02
FGF signaling pathway	29	1.13E-02
Glycolysis	11	4.44E-02
Integrin signaling	48	1.31E-06
Ubiquitin proteasome	34	1.45E-10
TCA cycle	7	6.14E-03
Pentose phosphate pathway	6	4.93E-02

Analyzed data from Pillai et al. (2019a).

Inhibition of Rock can increase blastocyst size

As proliferation is the prominent function for bTSCs during embryo elongation (Chang, 1952), and there are no previously known mechanisms associated with self-renewal of bTSC, we tested the effect of Rock inhibition on intact bovine blastocysts evaluating the effect on $CDX2^+$ cell numbers (Movie 1). Treatment of blastocysts with Rocki over a period of 48 h caused a large increase in embryo size, with both diameter and $CDX2^+$ cell numbers almost double those in controls (Fig. 1G). This result indicates a driving role for RhoA and Rock signaling in determining both trophoblast cell number and blastocyst size.

Inhibition of Rock promotes self-renewal in bTSCs

Self-renewal is crucial for the sustenance of bTSCs through developmental stages such as embryo elongation prior to implantation. To fully define the effects of Rocki on bTSCs and test for self-renewal, we examined both morphology and transcriptomics of the proliferating trophectodermal cells. With Rocki, trophoblast outgrowths on iMEFs could be successfully passaged repeatedly without loss of morphological characteristics and specific marker expression (Fig. 2A; Fig. S1). These cultures formed trophocysts, which are blastocyst-like structures without the inner cell mass (ICM) that is characteristic in bTSC cultures (Pillai et al., 2019a). Moreover, in the presence of Rocki, the proliferating trophoblasts were not dependent on the presence of iMEF feeders. When passaged onto cell culture dishes with no substrate provided, shredded colonies could effectively attach and survive only in the presence of Rocki, but not in its absence (Fig. 2B). Colonies expanded identically to cells on iMEFs with Rocki, and could be repeatedly passaged (more than 50 passages) and survive freeze-thaws without any morphological changes or changes in the ability to form trophocysts (Fig. S2), indicating that their functional identity is preserved. In contrast, the few feeder-free colonies that formed without Rocki grew very slowly, and culminated in prolonged arrest and eventual death.

We performed RNA-seq to study possible transcriptome changes that occur with prolonged culture of trophoblasts in Rocki (continuous treatment over four passages, ∼21 days) compared with early outgrowths of undifferentiated blastocyst-derived trophoblasts, as previously defined (Pillai et al., 2019a). There was a clear difference in clustering between the controls, Rocki in the presence of iMEF feeders and Rocki without feeders (Fig. 2C). Nevertheless, prolonged culture in the presence of Rocki did not affect bTSC marker expression irrespective of the presence or absence of feeders (Fig. 2D), suggesting that cells in both types of cultures undergo self-renewal without differentiation.

Development (2022) 149, dev200115. doi:10.1242/dev.200115

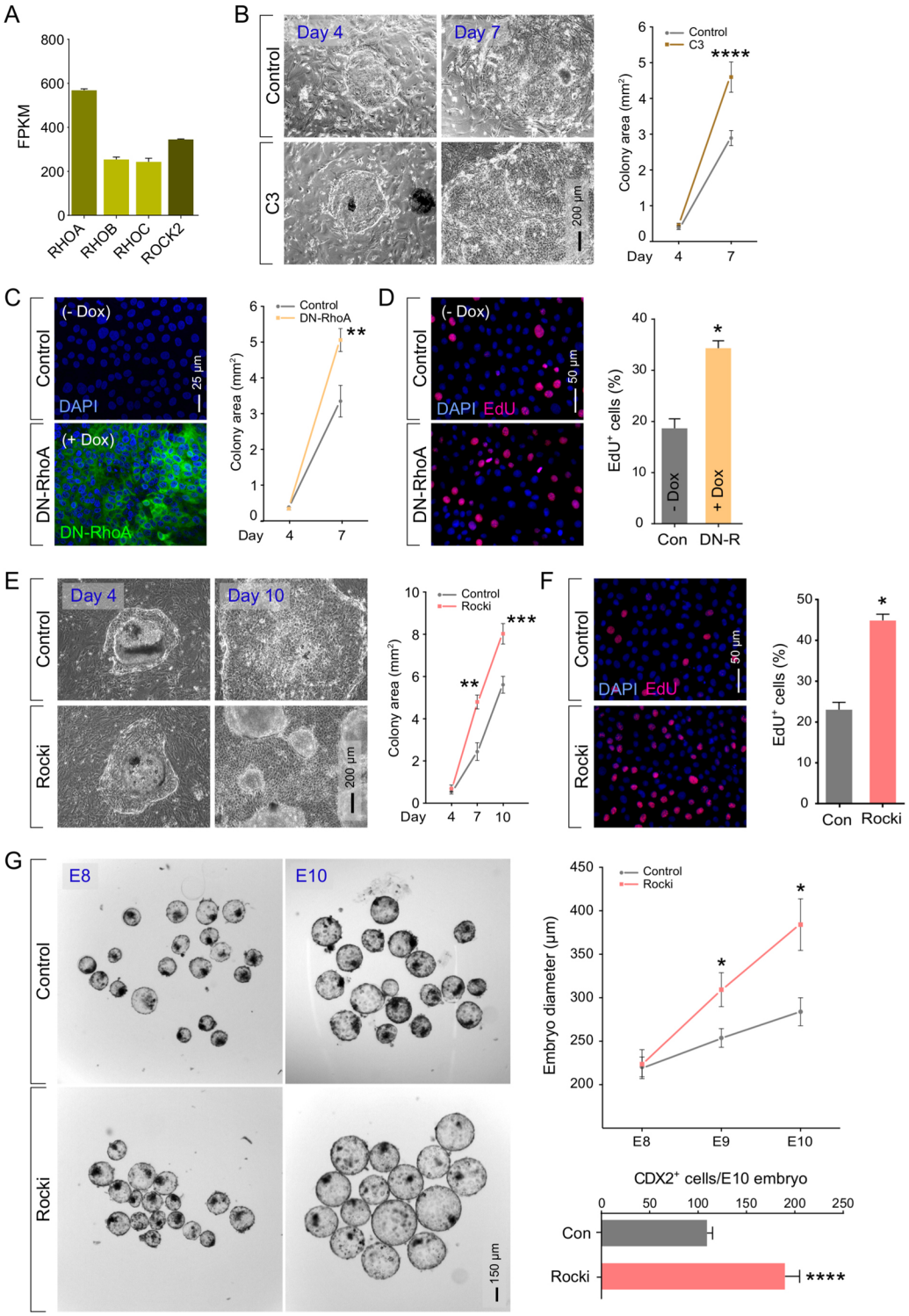

Fig. 1. Inhibition of RhoA and Rock signaling enhances proliferation of bovine TSCs. (A) RHOA, RHOB, RHOC and ROCK2 show moderate to high expression in primary blastocyst-derived trophectoderm outgrowths. (B) Early trophectoderm cultures on iMEFs showed significant increases in average colony area after treatment with a Rho A inhibitor (C3 transferase, 0.25 µg/ml) for 3 days compared with controls (n=6/group; ****P<0.0001). (C) Overexpression of a GFP-tagged dominant-negative mutant of RhoA (DN-RhoA; inducible by doxycycline/Dox) for 3 days caused significant increases to trophectoderm colony areas compared with controls (n=6/group; **P<0.01). (D) Overexpression of DN-RhoA also resulted in an increase in cells labeling positively for EdU in trophectoderm colonies compared with controls (*P<0.05), indicative of increased proliferation. (E) Early trophectoderm cultures on iMEFs showed significant increases in average colony area after treatment with a Rho kinase inhibitor/Rocki (Y-27632, 10 µM) for 3 (n=8/group; **P<0.01) and 6 days (n=8/group; ***P<0.001) compared with controls. (F) Rocki treatment also resulted in increase in cells labeling positively for EdU in trophectoderm colonies compared with controls (*P<0.05), which is indicative of increased proliferation. (G) Representative images from an experiment showing intact bovine blastocysts as controls or in the presence of Rocki, showing growth over 2 days in culture. Measurements of individual blastocyst diameters showed significant increases to the trophectoderm and blastocyst size after treatment with Rocki for 1-2 days compared with controls (*P<0.05), without any loss of morphology. Numbers of CDX2$^+$ cells also showed a significant increase after Rocki treatment for 2 days compared with controls (n>20/group; ****P<0.0001), indicating undifferentiated expansion.

Development (2022) 149, dev200115. doi:10.1242/dev.200115

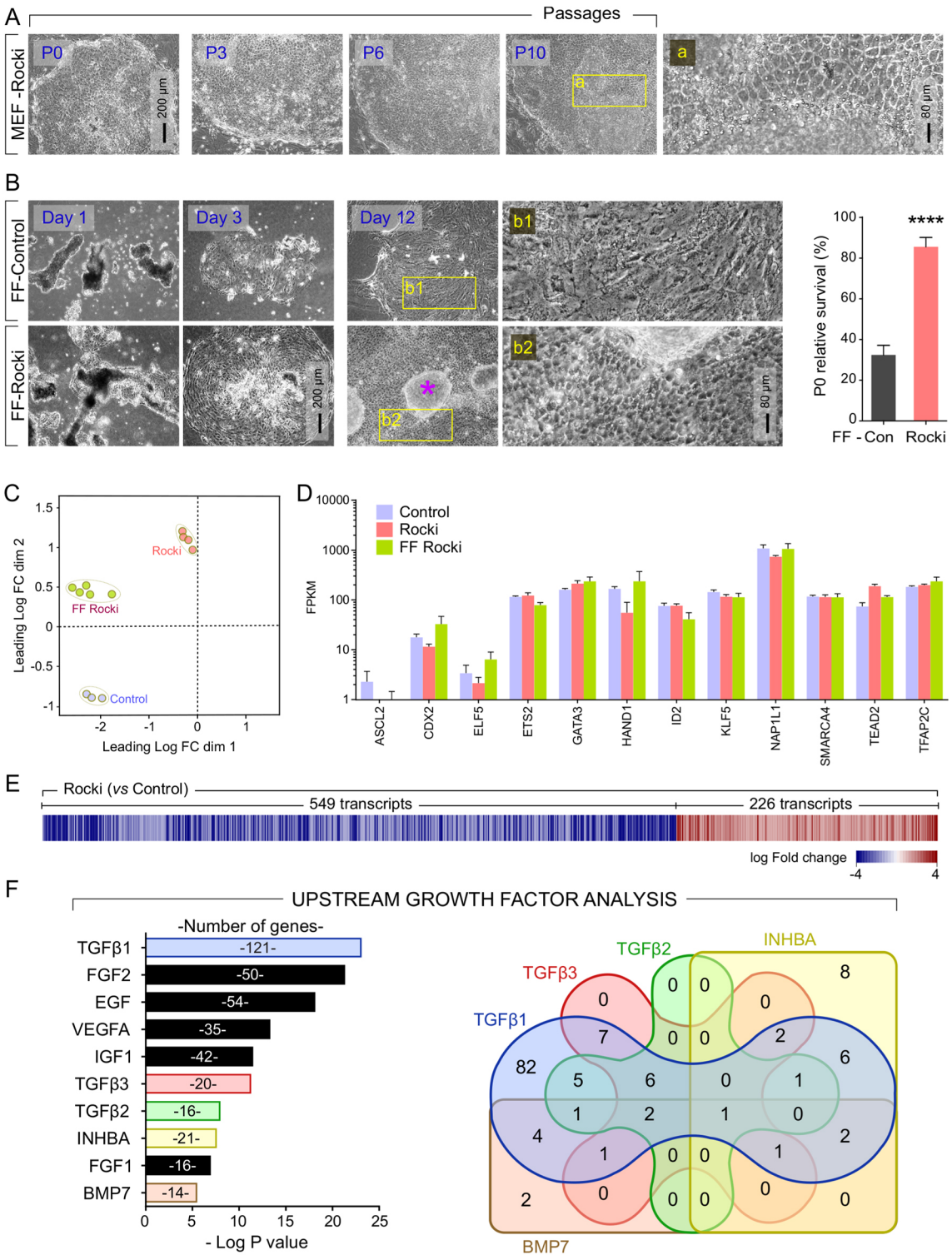

Fig. 2. Inhibition of Rho kinase maintains self-renewal in bovine TSCs, exposing mechanisms that induce differentiation. (A) Rocki enables long-term culture of primary blastocyst-derived TSC colonies on iMEFs without loss of morphological characteristics. (B) Rocki enables feeder-free culture of TSCs. Passaged colonies without iMEFs could effectively attach and survive, but only in the presence of Rocki (n=6/group; ****P<0.0001). Colonies cultured without Rocki show loss of the characteristic polygonal cell shape and prominent cell adhesions, suggestive of differentiation. Asterisk shows a trophocyst in development. (C) Multidimensional scaling plot of transcriptome datasets for: TSCs cultured on iMEFs with Rocki (n=4) or in feeder-free Rocki (n=5); and early outgrowths of undifferentiated blastocyst-derived trophoblasts on iMEFs (n=3), showing distinct cluster patterns. Within each group, biological replicates clustered together indicate similarity in gene expression profiles. (D) Expression of core TSC transcription factors in cells grown under the aforementioned conditions from mRNA sequencing. Data indicate that prolonged culture in the presence of Rocki did not impact TSC marker expression. (E) Heatmap showing differences to global gene expression observed in controls, indicative of shifts associated with spontaneous differentiation observed without Rocki. (F) Upstream growth factor analysis of genes upregulated in controls versus Rocki, which likely represent spontaneous differentiation. Results indicate that several members of the TGFβ superfamily were enriched (in colors), with TGFβ1 being the predominant growth factor involved in affecting 121 genes associated with spontaneous differentiation.

Development (2022) 149, dev200115. doi:10.1242/dev.200115

TGFβ1 signaling is the predominant pathway upstream of RhoA and Rock

To investigate signaling associated with differentiation, we used an integral feature in the controls, that the early trophoblast outgrowths are quite unstable and undergo spontaneous differentiation with survival lasting only for a few passages (Pillai et al., 2019a). As Rocki treatment allowed self-renewal that promoted long-term growth, even under feeder-free conditions, we reverse analyzed gene expression differences to understand the control as a means to detect mechanisms that induce spontaneous differentiation of bTSCs. This inverse three-way analysis integrating transcripts upregulated and downregulated by Rocki (Fig. 2E; Fig. S3; Table S1, sheet I), allowed us to simultaneously delineate the influence of iMEFs and focus on expression associated with differentiation signaling. Upstream growth factor analysis of the differentially downregulated genes (in response to Rocki) identified TGFβ1 as the predominant pathway involved in affecting gene expression associated with differentiation (Fig. 2F). Other receptors identified in the top 10 were enriched by less than 50% of that observed for TGFβ1. Moreover, the top 10 included other members of the TGFβ superfamily, such as TGFβ3, TGFβ2, INHBA and BMP7. On this basis, we hypothesized that TGFβ1 signaling was upstream of Rock, and tested whether treatment with TGFβ1 could affect stemness in bTSCs.

Expression of TGFβR1 and TGFβR2 were both observed in bTSCs (Fig. 3A; Fig. S4). Treatment of blastocyst-derived TSC outgrowths with SB431542/TGFβRi resulted in (1.75-fold) higher bTSC colony size at 3 days, which was identical to that observed with Rocki (1.75-fold), compared with controls (Fig. 3B). But by 6 days, bTSC colony sizes showed a modest yet significant increase in Rocki (1.72-fold) than in TGFβRi (1.5-fold) compared with controls (Fig. 3B). Treatment with TGFβ1 strongly suppressed proliferation of bTSCs; this effect could be partially reversed by addition of Rocki together with TGFβ1 (Fig. 3C). These findings provided the first direct evidence that Rock was an effector of TGFβ1 signaling in bTSCs. The precipitous decline in proliferation caused by TGFβ1 and the reversal by Rocki could be observed in time-lapse capture of cell growth and proliferation (Fig. 3D; Movie 2).

TGFβ1 signaling directs bTSC differentiation

Beyond the barrier presented to proliferation, significant shifts in cell morphology could be observed in bTSCs after exposure to TGFβ1. The first observation was that cells tended to become larger (occupying more surface area), with changes observed to cell-cell boundaries (Fig. 4A), suggesting an associated functional change. Cytokeratin and actin staining revealed extensive reorganization of the cytoskeletal framework in cells after TGFβ1 treatment, in both the cytosolic regions and the membrane skeleton (Fig. 4A; Fig. S5). Another significant observation was the appearance of a population of diplokaryotes/binucleate cells (BNCs; Fig. 4A); the overall ratio of BNCs to single-nucleated cells (SNCs) was significantly higher after TGFβ1 treatment (Fig. 4B). These BNCs were largely restricted to a peripheral zone in the trophoblast colonies. In previous literature, BNCs have been indicated as a hallmark of bovine trophoblast differentiation (Greenstein et al., 1958; Wooding, 1992). From our results, it was clear that Rocki even suppressed the formation of spontaneous BNCs in controls (Fig. 4B).

We then performed RNA-seq comparisons to gain a fuller understanding of the effects of TGFβ1 on bTSCs and the resulting morphological changes that were consistent with differentiation. We observed consistent upregulation of genes reported in differentiated cells and downregulation of genes reported to be expressed in bTSCs during the elongation stage (Fig. 4C). By contrasting the effects of Rocki with TGFβ1, an integrative analysis uncovered the mechanisms that balance self-renewal versus differentiation in bTSCs (Fig. 4D; Fig. S6; Table S1, sheet II). Distinct cellular pathways promoted self-renewal versus differentiation of bTSCs. By capturing receptor-based signaling, it was classified that the pathway mediated by decapentaplegic (DPP) and screw (SCW), two BMP family members, and the nicotinic acetylcholine receptor (nAch) were primary contributors to self-renewal signaling in bTSCs. Signaling in differentiated trophoblasts was diverse, perhaps reflecting the multifarious functions assumed by the differentiated placenta. It included responses to different cytokines (IL6, TNF, CCL2, CXCL5, CXCL2, TGFB1, INHBB, LIF, VEGFC and IL1A), and prominent developmental and immune signaling [Hedgehog signaling, toll-like receptors (TLR), NOD-like receptors, T-cell receptors (TCRs) and cytokine receptor interaction].

Transcriptional underpinnings of the TGFβ1 response

Separating genes upregulated by TGFβ1 treatment and clustering to visualize relative expression in TGFβ1 combined with Rocki treatment revealed three prominent clusters (Fig. 5A; Table S1, sheet III). Cluster I represented genes that were upregulated by TGFβ1 treatment even in the presence of Rocki treatment (Independent). Clusters II and III represented genes that were upregulated by TGFβ1 treatment but were moderately (Dependent^{lo}) or completely (Dependent^{hi}) reversed by Rocki treatment, respectively. Analysis for transcriptional regulators upstream of the differential expression observed with TGFβ1 treatment revealed candidates that were significantly enriched (Fig. 5B). Analysis of protein-protein interactions indicated that these enriched transcription factors were part of a regulatory network (Fig. 5C). In this list, we observed five upregulated by TGFβ1 that showed reversal of expression when combined with Rocki (TFAP2A, JUNB, NFKB1, NFKB2 and RELA), indicating direct downstream target actions of Rock (Fig. 5D). Four were downregulated by TGFβ1 with little reversal of expression when combined with Rocki (SP1, ATF2, TP53 and STAT1), and two were upregulated without reversal of expression when combined with Rocki (FOS and JUND) (Fig. 5D). There were signs of genomic instability with differentiation that was particularly apparent in BNCs (Fig. S7); such acquired abnormalities could contribute to irreversible shifts with differentiation. Furthermore, on examining the role of NFKB1 and NFKB2 as the highest induced reversible factor in bTSC differentiation, we uncovered its crucial role in differentiation. Treatment with a RelA inhibitor resulted in rapid cell death in TGFβ1-treated cells but not in Rocki controls (Fig. 5E; Movie 3). Such a result indicates a vital role for NFKB signaling in the survival of differentiated trophoblasts.

Rock activation alone can induce morphological differentiation in bTSCs

As Rocki promotes self-renewal, we examined the specific Rock-induced effects on bTSC to understand the trigger and early events in differentiation. By expressing a doxycycline-inducible constitutively active form of bovine ROCK2 (cRock2) in bTSCs, we discovered that cRock2 alone could bring about phenotypic changes observed with differentiation (Fig. 6). Induction of cRock2 was associated with a shift in cell

Development (2022) 149, dev200115. doi:10.1242/dev.200115

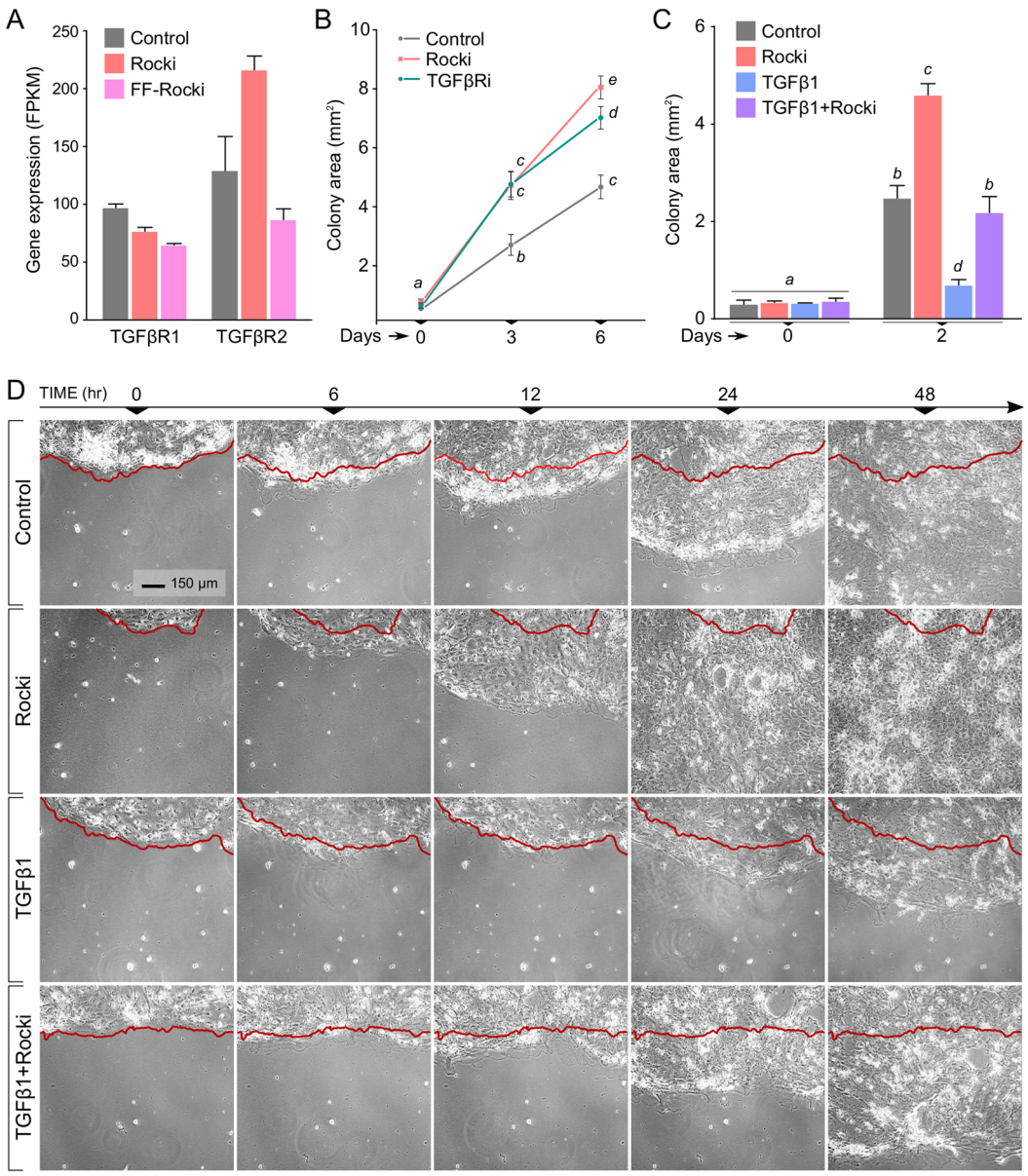

Fig. 3. TGFβ1 substantially suppresses growth of bovine TSC colonies, an effect that is reversed by inhibition of Rho kinase. (A) Both TGFβR1 and TGFβR2 are expressed in bTSCs, and are maintained at or above baseline levels in the presence of Rocki. (B) Inhibition of TGFβR (TGFβRi) enhanced proliferation of bTSCs; the effect was similar to Rocki treatment for the first 3 days, but significantly lower at 6 days. Data points with different letters indicate significant differences (n=10/group; P<0.05). (C) Treatment with TGFβ1 suppresses proliferation of bTSCs that inhibit colony growth; this effect is completely reversed to control levels with concurrent Rocki treatment, but remains lower than growth seen with Rocki treatment alone. Bars with different letters indicate significant differences (n=11/group; P<0.05). (D) Time-lapse images showing bTSC colony growth under different treatments showing rapid proliferation in Rocki treatment and suppression with TGFβ1. Rocki treatment could reverse TGFβ1 effects towards control levels. Red line is the reference TSC colony boundary at 0 h shown across all time points to indicate the extent of colony growth.

morphology, which included the appearance of a subpopulation of binucleate cells (Fig. 6A-C). Beyond the appearance of BNCs, we sporadically observed that cRock2 expression caused formation of a few multi-nucleated cells (MuNCs) that contained as many as 6-10 nuclei (Fig. 6A). Such MuNCs were also found occasionally in cells treated with TGFβ1 (Fig. 6D). We also observed a precipitous decline in proliferation rate with cRock2 (Fig. 6E) similar to that observed for TGFβ1 treatment.

Given the complexity of placental organogenesis in cattle, we looked for morphological patterns and dispersal of SNCs, BNCs and MuNCs in the *in vivo* differentiated/mature 70- to 80-day-old placenta. Histological examination of the placentomes and the inter-placentome regions indicated the diversity of interfaces/microenvironments formed by differentiated SNCs and the distribution of BNCs (Fig. 7). Binucleate cells could be seen in both the inter-placentome regions and in the placental regions within the placentome caruncular labyrinth. Albeit rare, we also observed the presence of MuNCs in the placentome (Fig. 7). A distinctive feature in all BNCs, MuNCs and some SNCs was their relatively larger size and an appearance of being ensconced in a circular space, suggesting a permissive extracellular matrix. We differentiate the subset of morphologically distinct larger SNCs using the term ‘giant’ SNCs (gSNCs).

Development (2022) 149, dev200115. doi:10.1242/dev.200115

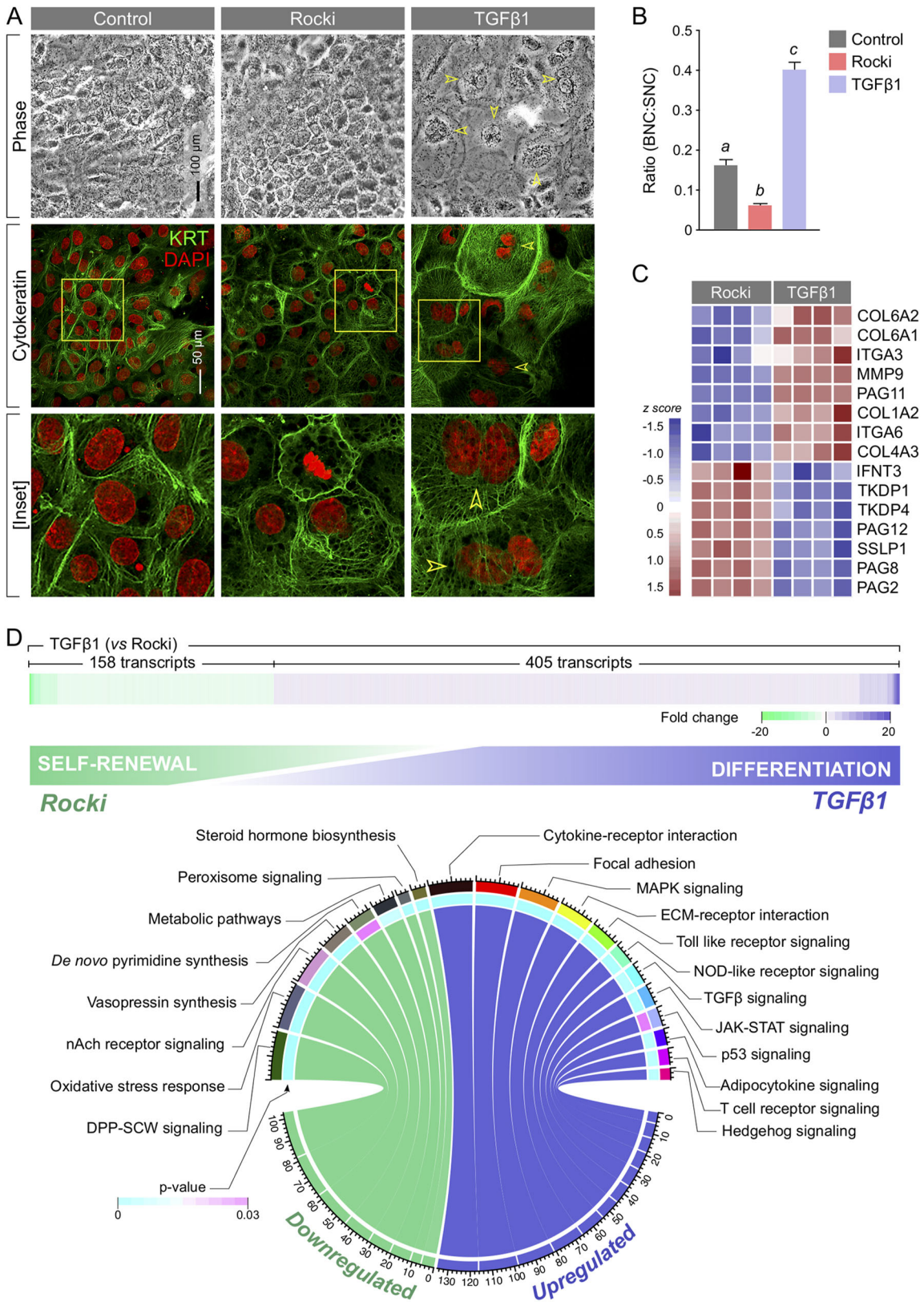

Fig. 4. TGFβ1 treatment induces differentiation of bovine TSCs. (A) Treatment with TGFβ1 induces substantial morphological changes that are consistent with differentiation in bTSCs. Representative phase contrast and immunohistochemistry images showing the observed increases in cell size, cytokeratin (KRT) reorganization and appearance of a subpopulation of binucleated cells (BNCs/arrowheads). (B) Treatment with TGFβ1 significantly increased the ratio of BNCs to single nucleated cells (SNCs) compared with baseline/control (spontaneous differentiation). Treatment with Rocki significantly decreased BNCs compared with controls. Bars with different letters indicate significant differences (n=8/group; P<0.05). (C) Expression of known target genes associated with TSC differentiation were consistently upregulated or downregulated with TGFβ1 treatment. (D) Examining the full profile of genes differentially regulated by TGFβ1 under feeder-free conditions could specifically delineate active signaling and functional mechanisms that sustain self-renewal and emerge with differentiation of bTSCs.

Development (2022) 149, dev200115. doi:10.1242/dev.200115

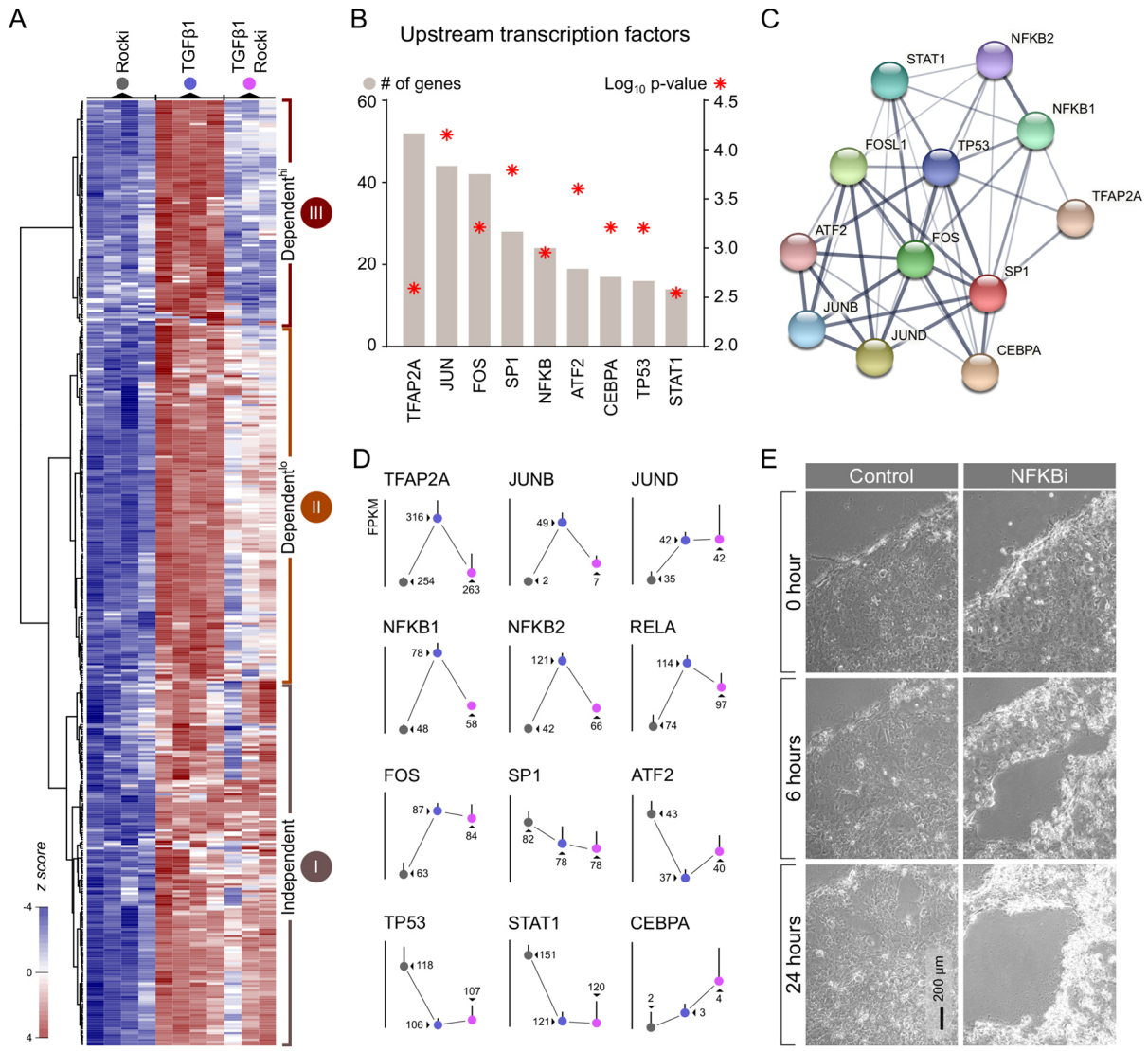

Fig. 5. RhoA- and Rock-dependent and -independent paths to transcriptional outcomes in TSC differentiation by TGFβ1. (A) Transcription factors significantly upregulated by TGFβ1 in bTSC differentiation formed three distinct clusters when aligned to concurrent treatment with TGFβ1 and Rocki, indicating RhoA- and Rock-dependent (hi), partially dependent (lo) and -independent clusters. (B,C) Evaluation of upstream transcription regulators responsible for gene expression changes in bTSCs induced by TGFβ1 indicated nine prominent/enriched transcription factors. Analysis of protein-protein interactions showed the network formed by these transcription factors relevant to systems interpretation of differentiation functions (line thickness indicates the strength of data support). (D) Gene expression levels for the identified upstream regulators could be categorized based on change in expression with treatments as RhoA- and Rock-dependent (either as high/hi or low/lo) or -independent mechanisms. Treatment indicated by colors as shown in A. (E) Of particular interest was NFKB, an essential mediator of inflammatory responses, unfamiliar to physiological regulation in trophoblast biology. Inhibition of NFKB-mediated transcription in bTSCs resulted in fragmentation and collapse of colonies (time-lapse images).

Differentiated trophoblasts allow for altered embryo-maternal interactions

In delineating transcripts encoding proteins secreted into the extracellular space that are increased with bTSC differentiation (Fig. 5A), we identified 51 significantly upregulated candidates that represented diverse communicatory functions (Table 2). With concurrent treatment with TGFβ and Rocki, it was identified that expression of 20 transcripts was reversible to almost baseline levels (Dependent^{hi}), 11 were partially reversible (Dependent^{lo}) and 20 remained unaffected by the addition of Rocki (Independent). This result is indicative of a notable shift to secretory functions associated with differentiation that possibly encompasses forward signaling mechanisms relevant to implantation (Fig. S8). Moreover, significant changes were also observed in the repertoire of membrane receptors expressed by differentiated trophoblasts (Fig. S9). These changes suggest a modification to extracellular responses and signaling that might be relevant for regional specializations that include interactions at the sites of implantation/placentomes.

DISCUSSION

Common to all eutherian mammals, proliferating TSCs ensure pregnancy success by defining preimplantation trophectoderm development and placental organogenesis. Previously, murine (Tanaka et al., 1998) and human (Okae et al., 2018) TSCs have been derived and used as models for studying placental function that represents an invasive hemochorial uterine association. In ruminants, the non-invasive epitheliochorial uterine association in

Development (2022) 149, dev200115. doi:10.1242/dev.200115

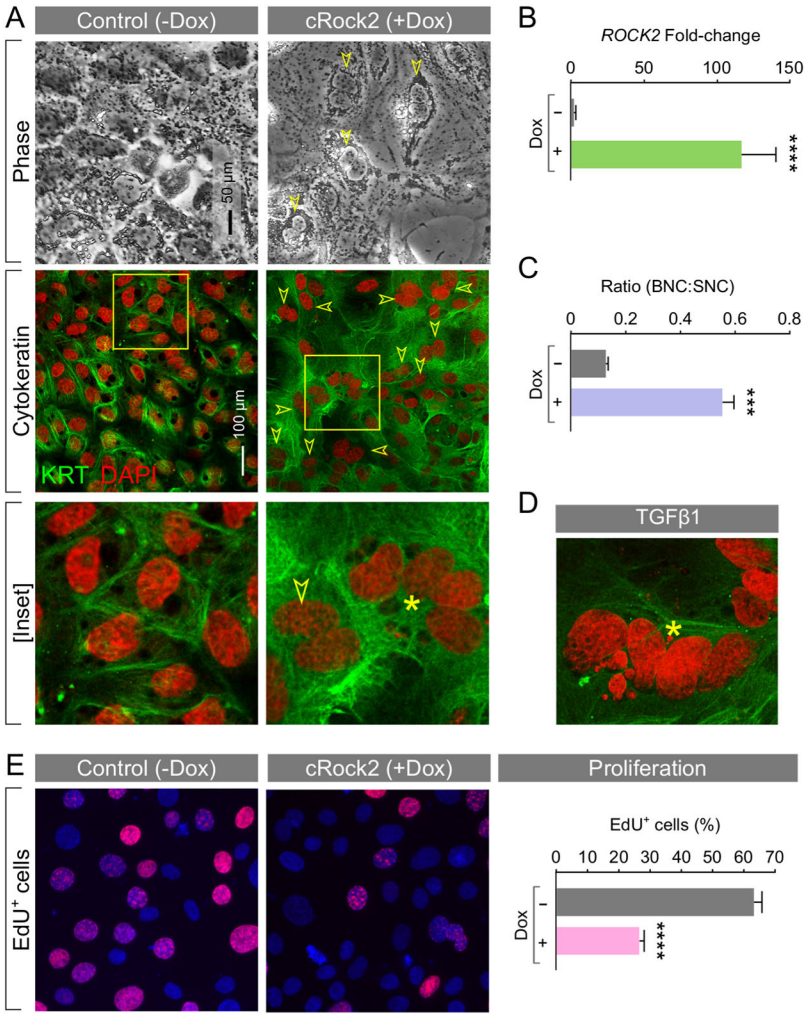

Fig. 6. Induced expression of constitutively active Rock2 results in changes consistent with differentiation. (A) Induced constitutively active Rock2 resulted in morphological changes similar to TGFβ1 treatment such as increases to cell size, cytokeratin (KRT) reorganization and appearance of binucleated cells (BNCs/arrowheads). Frequent multinucleated cells (MuNCs, asterisk) also appeared with TGFβ1 treatment. Representative phase contrast and immunohistochemistry images are shown. (B) Rock2 mRNA levels were significantly higher after induced expression of the constitutively active cRock2 transgene (****P<0.0001). (C) The ratio of BNCs to single nucleated cells (SNCs) was significantly increased with cRock2 expression (n=9/group; ***P<0.001). (D) MuNCs were also observed in response to TGFβ1 treatment of bTSCs, but were rare. (E) Induced cRock2 in bTSCs suppressed proliferation as measured by EdU labeling. This was consistent with observations made in TGFβ1-induced differentiation. Percentage of EdU-incorporated nuclei were significantly lower in cRock2-induced cultures (n=6/group; ****P<0.0001).

the form of cotyledonary placenta, presents a unique model that TSCs have yet to be derived/sustained successfully. Previously, we defined the physiological state of undifferentiated bTSCs by equating to the trophectoderm (TE) of blastocysts (Pillai et al., 2019a). By dissecting the pathways that trigger spontaneous differentiation of these cells, we now report that the attenuation of the RhoA and Rock signaling sustains self-renewal and promotes growth in bTSCs. Using methods that inhibit RhoA and Rock, bTSCs could be cultured upwards of 50 passages with minimal to no spontaneous differentiation, even under feeder-free conditions. This result is different from known mechanisms and conditions established for sustaining murine TSCs that require activation of fibroblast growth factor 4 (FGF4) signaling (Tanaka et al., 1998), and for sustaining human TSCs that require activation of wingless/integrated (WNT) and epidermal growth factor (EGF) pathways (Okae et al., 2018).

In intact blastocysts, inhibition of Rock dramatically increased embryo size and bTSC numbers, indicating that this mechanism is robust and could be a key determinant of preimplantation development in cattle. Recently, it has been reported that blastocyst size is dependent on hydraulic control by the blastocoel fluid (Chan et al., 2019). In identifying a role for RhoA and Rock signaling, a known remodeler of the cortical cytoskeleton (Ridley and Hall, 1992), our findings significantly add to this model, which is based on mechano-sensing and cortical tension in trophectodermal cells. It is conceivable that Rock inhibition alters the threshold for the hydraulically gated oscillations that would occur in the embryo. Nonetheless, our results present a parallel model in that control of mitotic rate in TSCs, perhaps also directed by cortical tension and RhoA and Rock signaling, is a fundamental regulator of blastocyst size.

Similarly, reliance on physical cues to balance proliferation has been demonstrated for primary human keratinocytes that reside in the epidermis (Kenny et al., 2018). Rho-Rock signaling in these cells has been associated with differentiation; inhibition of Rock increased proliferation (McMullan et al., 2003). Although this result is in agreement with our finding in bTSCs, it is in contrast to numerous other cell types in which Rho-Rock signaling has been reported to promote proliferation (Provenzano and Keely, 2011) and tumorigenesis (Kümper et al., 2016; Rath and Olson, 2012). Thus, the signaling mechanisms for RhoA and Rock can be significantly diverse (Etienne-Manneville and Hall, 2002) and also conditional to cell type, perhaps linked to structural contexts of the cellular niche (Julian and Olson, 2014).

There also appears to be species specificity regarding Rock signaling and the genesis of the blastocyst trophectoderm. Rho-Rock signaling via the Hippo pathway-YAP/TAZ activation has been shown to play a crucial role in murine and porcine trophectoderm (TE) specification; Rocki has been reported to suppress CDX2$^+$ cells (Kono et al., 2014; Liu et al., 2018). But in bovine development, Rocki has been reported to modestly increase the number of TE cells (Negrón-Pérez et al., 2018). The difference

Development (2022) 149, dev200115. doi:10.1242/dev.200115

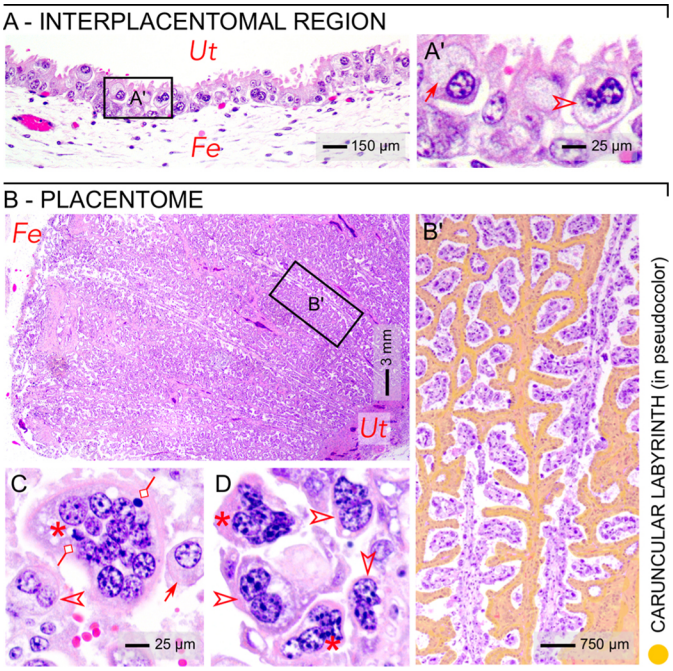

Fig. 7. Histomorphology of *in vivo* differentiated bovine trophoblasts corroborates *in vitro* morphological differentiation phenotypes. (A-D) Differentiated trophoblasts of the fetal chorion shown from a 70- to 80-day-old bovine placenta (Hematoxylin and Eosin staining). (A,A′) Representative interplacentomal region and inset showing the trophoblast layer [*Fe* represents the fetal side; *Ut* represents the uterine side] that consisted of single nucleated cells (SNC), some giant SNC (gSNC, arrow) and binucleated cells (BNC, arrowhead). (B,B′) Representative placentomal region and inset showing the existence of tortuous chorionic tubes seated within the uterine caruncular labyrinth (in B′, the maternal caruncle is pseudocolored to distinguish the fetal trophoblasts). Within the trophoblastic placentome unopposed to caruncular surfaces, two representative loci (C and D, from unmarked locations within B) show the presence of SNC, gSNC (arrow) and BNC (arrowheads) together with sporadic multinucleated cells (MuNCs, asterisks). Micronuclei (diamond headed lines in C) can be observed in MuNCs, which are indicative of genomic instability.

in regulation is consistent with the observation that CDX2 is essential only for TE maintenance, particularly in later embryonic stages in cattle (Berg et al., 2011); that TE specification might be delayed (Negrón-Pérez et al., 2017b), setting up a window of epigenetic plasticity that is prone to distortions by *in vitro* microenvironments. An extended period of epigenetic plasticity might explain the ability to grow TE-like cells that remain teratoma competent and express pluripotency markers such as NANOG together with CDX2, through inhibition of GSK3β and MEK with WNT activation (Huang et al., 2014). Inhibition of GSK3β and MEK has been used to sustain pluripotent stem cells (PSCs) in other species (Duggal et al., 2015; Ying et al., 2008); we recently discovered that sustenance of bovine-induced-PSCs/iPSCs require TGFβ/activin/nodal inhibition together with GSK3β and MEK inhibition (Pillai et al., 2019b, 2021). Nevertheless, pluripotent *in vitro* TE phenotypes neither represent the molecular signatures observed in the bovine blastocyst TE/primary bTSC outgrowths (Negrón-Pérez et al., 2017b; Pillai et al., 2019a) nor do they capture the true lineage of directed placental organogenesis. Our findings suggest that control of self-renewal in bTSCs is via an autoregulatory loop that can be sustained with the inhibition of differentiation using Rocki. Such a mechanism allows homogeneous expansion with some level of autonomy, such as that which occurs during embryo elongation (Betteridge et al., 1980; Clemente et al., 2009), and permits interaction with timely spatial signals from the uterus that direct region-specific differentiation, with contacts of implantation restricted to the caruncles (King et al., 1980).

Systems biology prediction of TGFβ1 signaling in bTSCs as an upstream regulator of RhoA and Rock is already supported by evidence in different contexts with different outcomes across several model systems (Bhowmick et al., 2003; Kamaraju and Roberts, 2005; Tian et al., 2003). In bTSCs, changes consistent with differentiation elicited by specific Rock2 activation corroborate this signaling relationship. It has been identified that TGFBR2 can directly phosphorylate the cell polarity regulator partitioning defective 6 (PAR6), which recruits SMURF2 to target RhoA (Ozdamar et al., 2005; Viloria-Petit et al., 2009). Another distinct mechanism for TGFβ1 signaling is via the activation of Smad signaling (Kawabata et al., 1999); SMAD3 was identified as one of the upstream transcriptional regulators involved in bTSC differentiation. Therefore, TGFβ1 signaling through SMAD3 could explain gene expression changes that were not reversed by Rocki and also why Rocki cannot completely reverse effects of TGFβ1 on TSC proliferation. Although this might appear as a bifurcated response to TGFβ1, there is also evidence for crosstalk. SMAD3 has been identified as a phosphorylation target (S203/207) for Rock downstream of TGFβ1 signaling (Kamaraju and Roberts, 2005). In mesenchymal stem cells, Rocki could significantly block SMAD phosphorylation associated with TGFβ1 signaling in a dose dependent manner (Xu et al., 2012). Therefore, it is plausible that exposure to physiologically regulated TGFβ1 levels (expected *in vivo*) might obviate any Rocki-independent effects. Another confounding *in vitro* factor is the known effect of serum in activating RhoA and Rock (Ridley and Hall, 1992). With serum being a necessary component in our medium, such an undesired effect could explain why TGFβRi alone is less effective for use in long-term bTSC sustenance. These considerations indicate that sustenance of bTSCs by Rocki alone, when there was no TGFβ1 added to the culture medium, is sufficient for a homeostatic balance in regulation.

In vivo, the uterus defines the sites of implantation (at caruncles forming a labyrinth) to form placentomes in cattle (Björkman, 1969). Such spatial and temporal uterine control is distinct from mouse and human models in which inductive stimuli from the blastocyst transform an arbitrary uterine site for implantation (Lopata, 1996). In this context, differentiation signals need to occur only after rapid bTSC expansion that occurs during embryo elongation in cattle (Chang, 1952), perhaps originating at the caruncular epithelium. There is already evidence for spatial regulation of differentiation in that TGFβ family proteins are found to be expressed in the uterine endometrium at the caruncular regions forming the placentomes (Hirayama et al., 2015; Munson et al., 1996), with TGFβ1 characteristically localized to the maternal septa within caruncles, and TGFβ2 and TGFβ3 localized to the caruncular uterine epithelium (Hirayama et al., 2015). Biological activation of TGFβ1 is known to be complex and tightly regulated in different systems, a mechanism that could provide temporal regulation. TGFβ1 is known to be produced in a latent form; an arginine-glycine-aspartic acid (RGD) motif interacts with several αV-class integrins, resulting in activation (Ludbrook et al., 2003; Munger et al., 1999). The essential nature of this activation is demonstrated in mice with a mutated RGD that display features similar to TGFβ1 knockout mice (Munger et al., 1999). Moreover, several latent TGFβ binding proteins (LTBPs) exist that are also required for functional activation and bioavailability of TGFβ1

Development (2022) 149, dev200115. doi:10.1242/dev.200115

Table 2. Transcripts coding for secreted proteins upregulated with TGFB1-induced differentiation

Gene	Protein	Fold Change	FDR	Cluster
LOXL2	Lysyl oxidase homolog 2	1.21	1.33E-21	Dependent^{hi}
TNXB	Tenascin XB	1.45	3.98E-25	Dependent^{hi}
PAG11	Pregnancy-associated glycoprotein 11	20.44	0	Dependent^{hi}
SFTPB	Pulmonary surfactant-associated protein	1.52	5.18E-06	Dependent^{hi}
WNT11	Wnt protein 11	1.49	3.31E-30	Dependent^{hi}
VWF	von Willebrand factor	1.21	1.74E-15	Dependent^{hi}
NPPB	Natriuretic peptides B	3.38	5.73E-17	Dependent^{hi}
INHBB	Inhibin β B chain	1.33	1.56E-07	Dependent^{hi}
BMP4	Bone morphogenetic protein 4	1.02	1.59E-16	Dependent^{hi}
WNT10A	Protein Wnt 10A	1.45	6.86E-06	Dependent^{hi}
LTBP2	Latent-transforming growth factor β	2.55	4.21E-28	Dependent^{hi}
LIF	Leukemia inhibitory factor	1.72	4.11E-05	Dependent^{hi}
SPP1	Osteopontin	4.98	9.29E-103	Dependent^{hi}
FSTL1	Follistatin-related protein 1	1.23	1.23E-11	Dependent^{hi}
LAMB3	Laminin subunit β3	2.54	2.26E-51	Dependent^{hi}
C8G	Complement C8 γ chain	1.37	4.72E-05	Dependent^{hi}
CRISPLD2	Cysteine-rich secretory protein	1.12	2.14E-25	Dependent^{hi}
BDNF	Brain-derived neurotrophic factor	2.22	7.99E-23	Dependent^{hi}
THBS1	Thrombospondin	1.25	3.57E-21	Dependent^{lo}
VWA7	von Willebrand factor A domain containing 7	1.26	6.33E-15	Dependent^{lo}
VEGFC	Vascular endothelial growth factor C	1.76	2.84E-29	Dependent^{lo}
MMP9	Matrix metalloproteinase 9	4.42	1.97E-139	Dependent^{lo}
COL1A2	Collagen α-2(I) chain	3.29	3.91E-17	Dependent^{lo}
TGFB1	Transforming growth factor β1	1.43	1.53E-23	Dependent^{lo}
IGFBP6	Insulin-like growth factor-binding protein 6	1.47	1.95E-34	Dependent^{lo}
SERPINE1	Plasminogen activator inhibitor 1	1.32	1.39E-52	Dependent^{lo}
SPINK1	Serine protease inhibitor Kazal type 1	2.88	1.32E-16	Dependent^{lo}
WNT5A	Wnt protein 5A	1.21	1.73E-05	Dependent^{lo}
SERPINB1	Leukocyte elastase inhibitor	1.08	0.00022	Dependent^{lo}
CATHL5	Cathelicidin-5	1.33	6.69E-08	Independent
SPON1	Spondin-1	1.57	2.46E-12	Independent
IGFBP2	Insulin-like growth factor binding protein 2	2.92	5.45E-17	Independent
MMP13	Collagenase 3	4.7	6.27E-24	Independent
LTBP1	Latent TGF-binding protein 1	1.09	8.80E-32	Independent
IGFBP3	Insulin-like growth factor binding protein 3	1.08	6.25E-22	Independent
TNC	Tenascin C	2.07	6.25E-62	Independent
ADAMTS3	ADAM metallopeptidase 3	2.23	4.06E-39	Independent
CCL2	C-C motif chemokine ligand 2	6.91	2.60E-58	Independent
CXCL2	C-X-C motif chemokine ligand 2	2.11	1.12E-11	Independent
SEMA3C	Semaphorin 3C	1.61	1.64E-12	Independent
PLAU	Urokinase-type plasminogen activator	1.97	1.19E-67	Independent
COL4A3	Collagen α3(IV) chain	2.41	2.05E-19	Independent
SERPINF2	α-2-antiplasmin	2.06	3.97E-16	Independent
CFB	C3/C5 convertase	1.37	6.84E-27	Independent
CXCL8	Interleukin 8	1.61	3.07E-09	Independent
IL6	Interleukin 6	1.37	1.78E-23	Independent

(Annes et al., 2004); they are covalently bound to the ECM (Saharinen et al., 1998), effectively tethering TGFβ1. Such region-specific restriction of signals could be appropriate for caruncular signals that direct implantation in cattle. From our data, bTSCs express several αV-class integrins (ITGAV, ITGA3, ITGB3, ITGB5 and ITGB6) and LTBPs (LTBP1, LTBP2 and LTBP3), indicating that they are poised to set up TGFβ1 activation and responses. Components for a similar TGFβ1 regulation reported as increasing adhesive properties at the conceptus-maternal interface have been identified in sheep (Jaeger et al., 2005).

This model for autoregulation of bTSC self-renewal in the absence of differentiation signals does not rule out the involvement of trophic factors and metabolites that might accelerate proliferation. The preimplantation embryo is exposed to endometrial secretions (Forde et al., 2014) and exosomal vesicles (Burns et al., 2018), within the uterine lumen, the full impacts of which remain to be dissected. Extending this model to differentiation in bTSCs, it is conceivable that spatial signals create divergent mechanisms between placentome and interplacentome regions. This introduces the concept of directed differentiation, to complement TGFβ, which might involve additional uterine inputs that shape final placental maturation. Transcriptional drivers of TGFβ1-induced early differentiation unraveled mechanisms that prime a diversity of morphological and functional changes. The AP-1 group of transcription factors that includes JUNB, JUND, FOS and ATF2 are known regulators of cellular functions, including differentiation (Shaulian and Karin, 2002). Among these, JUNB is not only known to be a negative regulator of cell proliferation (Passegué and Wagner, 2000) but is also involved in triggering mitotic defects that may cause genomic instability, which includes multinucleated cell formation (Farràs et al., 2008). In parallel, mechanisms such as those mediated by TP53, which is known to induce apoptosis in cells that encounter genetic anomalies (Lane, 1992), are suppressed, whereas factors like NFKB that regulate transcription of anti-

Development (2022) 149, dev200115. doi:10.1242/dev.200115

apoptotic genes and promote survival (Liu et al., 1996) are enhanced. Factors such as TFAP2A (Depoix et al., 2014) and CEBPA (Bamberger et al., 2004) have already been linked to placenta-expressed targets. Moreover, expression of components involved in differentiation [such as intronic Fematrin-1/BERV-K1 (FAT2; Nakaya et al., 2013)] was upregulated 2.6-fold, whereas others [such as placental lactogen (Duello et al., 1986)] were not regulated by the TGFβ1-, RhoA- and Rock-induced differentiation alone. From our analysis, it is evident that receptors upregulated upon differentiation could mediate further signaling cascades for specialization during placentation in the uterine sub-niches.

As a new paradigm, RhoA and Rock signaling under mechano-sensing is particularly relevant to trophoblasts because of its natural collective cell behaviors. This includes formation of a diffusion barrier via tight junctions setting up a transtrophectoderm potential (Cross et al., 1973) and sheets of cells budding to form trophocysts (Pillai et al., 2019a), indicating a preference for hydraulic homeostasis. Cell-cell and cell-ECM adhesions are known to provide mechanical coupling, with biased force distribution to specific regions (Schaumann et al., 2018). It can be anticipated that such influences exist in bTSC colonies and affect RhoA and Rock signaling (Lessey et al., 2012; Ridley and Hall, 1992). Such forces perhaps explain why BNCs that appear with differentiation are roughly in a peripheral zone in these colonies. Radial traction force distribution, as observed for epithelial cell colonies (Zhang et al., 2019), could direct BNC formation in just the peripheral zone of differentiating bTSCs. We find that Rock2 activation alone can drive BNC formation; there is also evidence that mechanical forces/cortical tension activate latent TGFβ1 in cells (Giacomini et al., 2012), providing possible synergy between TGFβ1 and Rock in bTSC differentiation. This remains relevant in the *in vivo* context, as tethers established with the caruncles could act as focal points for high traction forces; BNCs have been observed to be enriched in the placentomal regions. This localization appears to be a relevant niche for BNCs as they have been linked to possible secretory functions (Wooding, 1992) and therefore benefit from immediate proximity to the maternal uterine epithelium. In this context, we have added new information identifying the growth factors/cytokines produced in differentiated bTSCs. These gene products indicate a variety of possible functions linked to autocrine and paracrine signaling that are relevant to setting up and maintaining the embryo-maternal interface. Although functional distinctions to MuNC formation are not clear, it is evident that they can emerge in both TGFβ1- and Rock-induced bTSC differentiation. In previous literature, MuNCs have been described as part of maternal giant cells of the maternal epithelium (King et al., 1980). Our results suggest that MuNCs can be formed by differentiated trophoblasts, which are distinct from the maternal epithelium.

In summary, we uncover fundamental mechanisms underlying bTSC self-renewal and differentiation (Fig. 8), that are highly relevant to developmental events, including blastocyst size, embryo elongation and placentation in ruminants. Our results point out some key differences between bTSCs and murine and human TSCs. Although similar Rock and TGFβ inhibition has been used in the cocktail developed for sustaining human TSCs, the crucial components appear to be wingless/integrated (Wnt) activation in the presence of epidermal growth factor (Okae et al., 2018). On the other hand, murine TSCs maintained with FGF4 can be supported by TGFβ, which has been shown to prevent differentiation (Erlebacher et al., 2004), in contrast to TGFβ driving differentiation in bTSCs. Our findings in systems biology coupled to both conserved and comparative understanding of mechanisms in bTSCs and placental development are poised to advance knowledge of trophoblast biology and its evolutionary path.

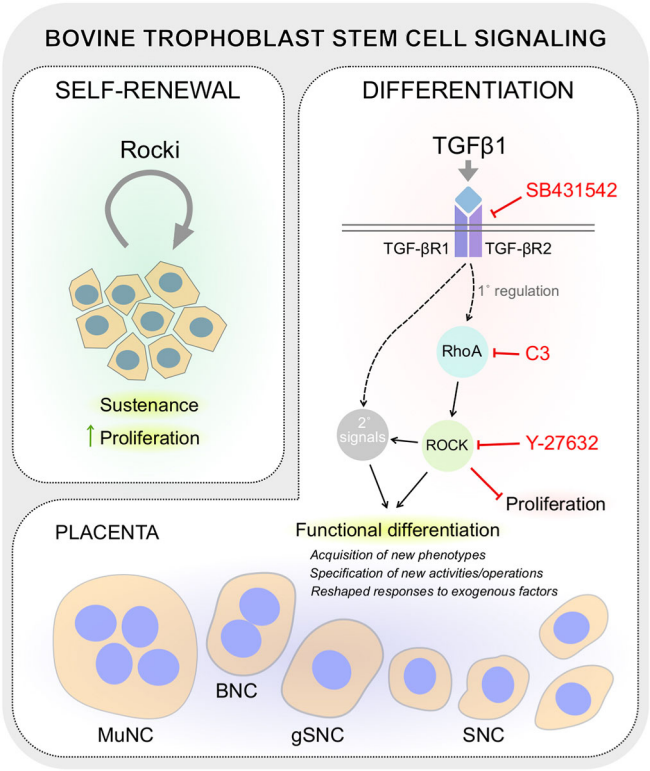

Fig. 8. Self-renewal and differentiation signaling in bTSCs. Bovine TSC expansion by self-renewal is achieved by attenuation of RhoA and Rock signaling. Proliferation accelerated via this mechanism could significantly increase blastocyst/embryo size. Differentiation is triggered by the induction of RhoA and Rock signaling through upstream TGFβ1 and TGFβR, resulting in morphological and functional trophoblastic features, as seen after placentation *in vivo*. This includes the specification of new characteristics and divergent responses to exogenous factors, which occurs simultaneously to a shift in cell phenotypes that includes multinucleated cells (MuNCs), binucleated cells (BNCs), single nucleated cells (SNCs) and giant single nucleated cells (gSNCs).

MATERIALS AND METHODS

Proteome and transcriptome pathways in bovine TSCs

Proteomics and transcriptomics datasets from undifferentiated blastocyst-derived trophectoderm outgrowths previously used to define baseline expression profiles of bovine TSCs (Pillai et al., 2019a) were analyzed for enriched pathways. The TSC proteome (MassIVE: MSV000083135) and the TSC transcriptome (NCBI: GSE122418) were subjected to gene enrichment and pathway analysis using the recently updated protein analysis through evolutionary relationships/PANTHER pathway prediction algorithm (Mi et al., 2021).

In vitro embryo production

Protocol for *in vitro* production of bovine embryos was as previously described (Negrón-Pérez et al., 2017a). In brief, follicles measuring 2-10 mm were sliced to obtain cumulus oocyte complexes (COCs) from ovaries collected at a local abattoir (Central Beef Packing Company in Center Hill, FL, USA). COCs with at least one complete layer of compact cumulus cells were selected, washed in oocyte collection medium and placed as groups of 10 in 50 µl drops of oocyte maturation medium overlaid with mineral oil. The COCs were matured for 20-22 h in a humidified atmosphere of 5% CO_2 at 38.5°C. After maturation, COCs were placed as groups of 50/well in four-well plates containing 425 µl of In Vitro Fertilization-Tyrode's Albumin Lactate Pyruvate (IVF-TALP) medium

Development (2022) 149, dev200115. doi:10.1242/dev.200115

(Caisson Labs), and 20 µl of 0.25 mM hypotaurine, 25 µM epinephrine and 0.5 mM penicillamine in 0.9% NaCl (w/v). Semen from frozen-thawed straws from three bulls were pooled, purified with ISolate [Irvine Scientific; 50% (v/v) and 90% (v/v)] and diluted to a final concentration in the fertilization dishes of 1×10^6/ml. Fertilization was allowed to proceed for 8-9 h in a humidified atmosphere of 5% CO_2 at 38.5°C. After fertilization, putative zygotes were denuded of cumulus cells by vortexing in 100 µl hyaluronidase (1000 U/ml in ∼0.5 ml HEPES-TALP) and cultured in groups of 25-30 in 50 µl synthetic oviduct fluid-bovine embryo 2 (SOF-BE2) in a humidified atmosphere of 5%, 5%, 90% (v/v) of CO_2, O_2 and N_2, respectively, at 38.5°C. Embryos that developed to blastocysts by 7 days after fertilization were used for trophoblast cultures.

Derivation and culture of trophectoderm outgrowths

Primary cultures of bovine trophectoderm colonies were established by plating hatched or zona removed (using 0.1% Pronase proteinase) day 7-8 blastocysts into 12-well culture dishes seeded with irradiated mouse embryonic fibroblast (MEF) feeders. Cultures were provided 1:1 mixture of Dulbecco's modified eagle medium (DMEM) and M199 containing 15% (v/v) fetal bovine serum, 1% (v/v) non-essential amino acids supplement and 1% (v/v) penicillin-streptomycin. All incubations were performed at 37°C under an atmosphere of 5% CO_2. Passage of TSC outgrowths was carried out by mechanical dissociation of primary colonies by forcing jets of culture medium using a 25 G needle. Sheets of primary colonies were broken up into smaller pieces by shear aspirations using a micropipette and then plated to 35 mm culture dishes with either MEF feeders or coated with 0.1% gelatin to generate secondary colonies. Culture medium was changed every 48 h until cells were confluent. Subsequent TSC passages were also continued via mechanical dissociation as described above.

Experimental treatments for TSCs and embryos

For TSC experiments, colonies were exposed to pharmacological inhibitors or growth factors: 2 µg/ml C3 transferase (Cytoskeleton), 10 µM Y-27632 (Enzo Life Sciences), 2 µM SB 431542 (Reagents Direct), 50 µM JSH-23 (Sigma) or 10 ng/ml recombinant human TGFβ1 (PeproTech). After treatment, cells were examined for morphology, prepared for immunostaining or harvested for total RNA extractions. For embryo experiments, IVF derived day 8 embryos (20-30 embryos per group) were cultured in low attachment 35 mm dishes with 1 ml of trophoblast medium supplemented with either 0 or 10 µM Y-27632. Embryos were collected after 24 or 48 h of treatment and either imaged to measure diameter or fixed for immunofluorescent differential cell counting using caudal type homeobox 2 (CDX2). For both TSCs and embryos, phase-contrast images were acquired using either a DFC365FX camera in M80 stereo or an ICC50HD camera in DMIL inverted microscopes (Leica). Measurement of embryo size was performed in perpendicular directions along the axis of symmetry and averaged for each embryo. Enumeration of $CDX2^+$ cells was performed by acquiring confocal *z*-stacks (Meta 510, Zeiss) followed by 3D reconstructions. For time-lapse microscopy, images were captured every 10 min using a Lumascope-720 microscope with a XYZ auto-stage placed in an incubator at 37°C and 5% CO_2. ImageJ software (Schneider et al., 2012) was used to quantify colony areas and cell numbers and for making measurements of acquired images.

Immunocytochemistry and histology

In preparation for imaging, TSCs were grown on glass coverslips and embryos were handled in suspension. All steps involved in immunolabeling TSCs and imaging have been previously described (Pillai et al., 2019a). Incubations were carried out using primary antibodies: a mouse monoclonal anti-cytokeratin antibody (Cell Signaling Technology; clone C11; 1:400) or with an affinity-purified mouse monoclonal antibody against caudal type homeobox 2 (CDX2, clone 88, BioGenex; ready to use). Alexa Fluor-conjugated secondary anti-mouse Fab′ fragments (Jackson Immunoresearch; 1:500) were used for labeling. For mounting, embryos were sandwiched between a slide and coverslip with Prolong Gold reagent (Life Technologies). For visualizing actin, TSCs were prepared as for immunocytochemistry and incubated with 50 µg/ml rhodamine-labeled phalloidin for 45 min at room temperature followed by washing coverslips before mounting. Images were acquired using a confocal microscope (Meta 510, Zeiss). For histological analysis, placentomes were dissected from material harvested immediately postmortem at ∼100 days of pregnancy, fixed in 4% formaldehyde and embedded in paraffin blocks. Thin sections (4 µm) were stained using a standard Hematoxylin and Eosin staining protocol (Morohaku et al., 2014).

5-Ethynyl-20-deoxyuridine (EdU) assay

Cell proliferation was quantified by an EdU incorporation assay using Click-iT EdU Alexa Fluor Imaging Kit (Life Technologies). Cells were incubated with 10 µM EdU for 12 h and EdU was visualized according to the manufacturer's instructions. In brief, cells were permeabilized in 0.5% Triton X-100 in PBS for 60 min, washed three times with 3% BSA in PBS and then incubated in the Click-iT reaction cocktail (containing buffer, $CuSO_4$ and Alexa Fluor Azide) for 1 h at room temperature. The reaction was then stopped by rinsing with PBS and samples were mounted for imaging.

Generation of expression constructs, viral production and transduction

To generate the pLenti-TRE-RTTA vector used for doxycycline-inducible gene expression, the CMV promoter of the pLenti-CMV-GFP-Puro [Addgene #17448 (Campeau et al., 2009)] vector was replaced with a doxycycline inducible minimal CMV promoter and the puromycin resistance gene was replaced by the RTTA element downstream of the PGK promoter by restriction cloning. The eGFP-RhoA-T19N and constitutively active bovine ROCK2 were PCR amplified from the teto-FUW-eGFP-RhoA-T19N [Addgene #73082 (Kong et al., 2013)] and pSILK CA ROCK2 [Addgene #84649 (Wong et al., 2015)] vectors, and were inserted in the pLenti-TRE-RTTA vector to generate doxycycline-inducible pLenti-TRE-RhoT19N-RTTA and pLenti-TRE-CA-ROCK2-RTTA vectors, respectively. pLenti-EF1α-GFP vector was constructed by replacing the CMV promoter of pLenti-CMV-GFP with an EF1α promoter and used to make control viruses. Lentiviral particles were produced in 293T cells by co-transfecting transfer vectors with helper plasmids encoding gag, pol and rev. Viral supernatants were collected at 48 and 72 h, pooled and filtered using 0.45 µm PES filters. Viruses were concentrated by ultracentrifugation at 25,000 ***g*** for 90 min before use. Trophoblast colonies were transduced by adding concentrated lentiviruses to the culture medium and incubating for 24 h. Control GFP vectors were used to estimate infection rates associated with viral preparation batches. TSCs were subsequently passaged and used for experiments.

Gene expression assays

Total cellular RNA was extracted using TRIzol (Life Technologies). Reverse transcription of 1.5 µg of total RNA was carried out with Oligo-dT using the Multiscribe reverse transcriptase (Life Technologies). Quantitative PCR (qPCR) was performed with the SYBR Green detection method to analyze expression using specific primers (Table S1, sheet IV) after confirming fidelity of amplification and efficiency. Expression data were normalized to glyceraldehyde 3-phosphate dehydrogenase (GAPDH). Relative quantification as fold-change was calculated using the $2^{-\Delta/\Delta Ct}$ method (Livak and Schmittgen, 2001).

Statistical comparisons

All statistical analyses were carried out using GraphPad Prism software. Statistical significance was determined using a one-tailed unpaired Student's *t*-test or one-way ANOVA. $P<0.05$ was considered significant unless otherwise specified. Data are mean±s.e.m.

Trophoblast transcriptomics and bioinformatic analysis

Total RNA was extracted from trophoblast colonies using RNAqueous micro kit (Thermo Fisher Scientific). Integrity was checked using the Bioanalyzer 2100 (Agilent Technologies), mRNA was isolated using poly(A) capture,

fragmented and cDNA library construction was performed using TruSeq stranded total RNA sample preparation kit (Illumina). Samples were provided with unique bar code sequences and pooled for sequencing by synthesis to obtain short single reads on a HiSeq4000 (Illumina). Reads were aligned to the bovine genome (ARS-UCD1.2) using Tophat (version 2.0.9) (Kim et al., 2013). Raw count for each gene was estimated with the BioConductor (EdgeR version 3.18.1) package using BAM files. Differentially expressed genes were identified using the DESeq package (Anders and Huber, 2010). Raw *P* values of multiple tests were corrected using false discovery rate (Benjamini and Hochberg, 1995). The transcriptomics and proteomics datasets were classified by using gene ontology (GO) terms using PANTHER (Mi et al., 2017) and DAVID (Huang et al., 2008) bioinformatic tools. GO terms and corresponding corrected *P*-values were used as input to perform a REViGO analysis to visualize semantic clustering of the identified top GO terms and reduce GO redundancy (Supek et al., 2011). The output plot was adjusted to highlight and annotate clusters of enriched GO terms. For integrated functional evaluation and upstream analysis of differentially expressed genes, the Ingenuity pathway analysis (IPA, Qiagen) algorithm was used to identify transcriptional regulators that account for the gene expression changes (Krämer et al., 2014). Regulatory networks evaluating protein-protein interactions were generated using the STRING database (Szklarczyk et al., 2021). Multidimensional scaling (MDS) plots were generated using the plotMDS function of edgeR after normalization using the trimmed mean of M-values (TMM) method (Robinson and Oshlack, 2010). Heatmap.2 and Circlize (gplots packages in R) were used to visualize data using heat maps and circos plots, respectively.

Acknowledgements
We thank W. Ronald Butler for being an enthusiastic supporter of our projects on the bovine embryo; over the years, we have tremendously gained from his anecdotes and insights.

Competing interests
The authors declare no competing or financial interests.

Author contributions
Conceptualization: V.V.P., V.S.; Methodology: V.V.P., T.G.K., S.G., V.S.; Formal analysis: V.V.P.; Investigation: V.V.P., T.G.K., S.G., M.D., L.G.B.S.; Resources: S.H.C., P.J.H., V.S.; Data curation: V.V.P.; Writing - original draft: V.V.P.; Writing - review & editing: V.S.; Visualization: V.S.; Supervision: V.S.; Project administration: V.S.; Funding acquisition: V.S.

Funding
This work was supported by start-up funds from the College of Agriculture and Life Sciences at Cornell University to V.S., and by L. E. 'Red' Larson Endowment funds to P.J.H.

Data availability
Complete RNA-seq datasets have been deposited in GEO under accession number GSE181252.

References
Anders, S. and Huber, W. (2010). Differential expression analysis for sequence count data. *Genome Biol.* **11**, R106. doi:10.1186/gb-2010-11-10-r106

Annes, J. P., Chen, Y., Munger, J. S. and Rifkin, D. B. (2004). Integrin αvβ6-mediated activation of latent TGF-β requires the latent TGF-β binding protein-1. *J. Cell Biol.* **165**, 723-734. doi:10.1083/jcb.200312172

Atkinson, B. A., King, G. J. and Amoroso, E. C. (1984). Development of the caruncular and intercaruncular regions in the bovine endometrium. *Biol. Reprod.* **30**, 763-774. doi:10.1095/biolreprod30.3.763

Aziz, M. and Alexandre, H. (1991). The origin of the nascent blastocoele in preimplantation mouse embryos ultrastructural cytochemistry and effect of chloroquine. *Roux Arch Dev Biol* **200**, 77-85. doi:10.1007/BF00637187

Bamberger, A.-M., Makrigiannakis, A., Schröder, M., Bamberger, C. M., Relakis, C., Gellersen, B., Milde-Langosch, K. and Löning, T. (2004). Expression pattern of the CCAAT/enhancer-binding proteins C/EBP-α, C/EBP-β and C/EBP-δ in the human placenta. *Virchows Arch.* **444**, 149-152. doi:10.1007/s00428-003-0935-7

Bazer, F. W. and Thatcher, W. W. (2017). Chronicling the discovery of interferon tau. *Reproduction* **154**, F11-F20. doi:10.1530/REP-17-0257

Bazer, F. W., Simmen, R. C. and Simmen, F. A. (1991). Comparative aspects of conceptus signals for maternal recognition of pregnancy. *Ann. N. Y. Acad. Sci.* **622**, 202-211. doi:10.1111/j.1749-6632.1991.tb37863.x

Benjamini, Y. and Hochberg, Y. (1995). Controlling the false discovery rate: a practical and powerful approach to multiple testing. *J. R. Stat. Soc. Ser. B* **57**, 289-300. doi:10.1111/j.2517-6161.1995.tb02031.x

Berg, D. K., Smith, C. S., Pearton, D. J., Wells, D. N., Broadhurst, R., Donnison, M. and Pfeffer, P. L. (2011). Trophectoderm lineage determination in cattle. *Dev. Cell* **20**, 244-255. doi:10.1016/j.devcel.2011.01.003

Betteridge, K. J., Eaglesome, M. D., Randall, G. C. B. and Mitchell, D. (1980). Collection, description and transfer of embryos from cattle 10-16 days after oestrus. *J. Reprod. Fertil.* **59**, 205-216. doi:10.1530/jrf.0.0590205

Bhowmick, N. A., Ghiassi, M., Aakre, M., Brown, K., Singh, V. and Moses, H. L. (2003). TGF-β-induced RhoA and p160ROCK activation is involved in the inhibition of Cdc25A with resultant cell-cycle arrest. *Proc. Natl. Acad. Sci. USA* **100**, 15548-15553. doi:10.1073/pnas.2536483100

Björkman, N. H. (1969). Light and electron microscopic studies on cellular alterations in the normal bovine placentome. *Anat. Rec.* **163**, 17-29. doi:10.1002/ar.1091630103

Burns, G. W., Brooks, K. E., O'Neil, E. V., Hagen, D. E., Behura, S. K. and Spencer, T. E. (2018). Progesterone effects on extracellular vesicles in the sheep uterus†. *Biol. Reprod.* **98**, 612-622. doi:10.1093/biolre/ioy011

Campeau, E., Ruhl, V. E., Rodier, F., Smith, C. L., Rahmberg, B. L., Fuss, J. O., Campisi, J., Yaswen, P., Cooper, P. K. and Kaufman, P. D. (2009). A versatile viral system for expression and depletion of proteins in mammalian cells. *PLoS ONE* **4**, e6529. doi:10.1371/journal.pone.0006529

Carter, A. M. (2012). Evolution of placental function in mammals: the molecular basis of gas and nutrient transfer, hormone secretion, and immune responses. *Physiol. Rev.* **92**, 1543-1576. doi:10.1152/physrev.00040.2011

Chan, C. J., Costanzo, M., Ruiz-Herrero, T., Mönke, G., Petrie, R. J., Bergert, M., Diz-Muñoz, A., Mahadevan, L. and Hiiragi, T. (2019). Hydraulic control of mammalian embryo size and cell fate. *Nature* **571**, 112-116. doi:10.1038/s41586-019-1309-x

Chang, M. C. (1952). Development of bovine blastocyst with a note on implantation. *Anat. Rec.* **113**, 143-161. doi:10.1002/ar.1091130203

Clemente, M., De La Fuente, J., Fair, T., Al Naib, A., Gutierrez-Adan, A., Roche, J. F., Rizos, D. and Lonergan, P. (2009). Progesterone and conceptus elongation in cattle: A direct effect on the embryo or an indirect effect via the endometrium? *Reproduction* **138**, 507-517. doi:10.1530/REP-09-0152

Cross, M. H., Cross, P. C. and Brinster, R. L. (1973). Changes in membrane potential during mouse egg development. *Dev. Biol.* **33**, 412-416. doi:10.1016/0012-1606(73)90146-2

Depoix, C. L., Debiève, F. and Hubinont, C. (2014). Inhibin alpha gene expression in human trophoblasts is regulated by interactions between TFAP2 and cAMP signaling pathways. *Mol. Reprod. Dev.* **81**, 1009-1018. doi:10.1002/mrd.22421

Duello, T. M., Byatt, J. C. and Bremel, R. D. (1986). Immunohistochemical localization of placental lactogen in binucleate cells of bovine placentomes. *Endocrinology* **119**, 1351-1355. doi:10.1210/endo-119-3-1351

Duggal, G., Warrier, S., Ghimire, S., Broekaert, D., Van Der Jeught, M., Lierman, S., Deroo, T., Peelman, L., Van Soom, A., Cornelissen, R. et al. (2015). Alternative routes to induce naïve pluripotency in human embryonic stem cells. *Stem Cells* **33**, 2686-2698. doi:10.1002/stem.2071

Erlebacher, A., Price, K. A. and Glimcher, L. H. (2004). Maintenance of mouse trophoblast stem cell proliferation by TGF-β/activin. *Dev. Biol.* **275**, 158-169. doi:10.1016/j.ydbio.2004.07.032

Etienne-Manneville, S. and Hall, A. (2002). Rho GTPases in cell biology. *Nature* **420**, 629-635. doi:10.1038/nature01148

Farràs, R., Baldin, V., Gallach, S., Acquaviva, C., Bossis, G., Jariel-Encontre, I. and Piechaczyk, M. (2008). JunB breakdown in mid-/late g 2 is required for down-regulation of cyclin A2 levels and proper mitosis. *Mol. Cell. Biol.* **28**, 4173-4187. doi:10.1128/MCB.01620-07

Finkel, H. S. (1931). The diagnosis of pregnancy by the Aschheim-Zondek test. *N. Engl. J. Med.* **204**, 203-209. doi:10.1056/NEJM193101292040503

Forde, N., McGettigan, P. A., Mehta, J. P., O'Hara, L., Mamo, S., Bazer, F. W., Spencer, T. E. and Lonergan, P. (2014). Proteomic analysis of uterine fluid during the pre-implantation period of pregnancy in cattle. *Reproduction* **147**, 575-587. doi:10.1530/REP-13-0010

Gey, G. O., Seegar, G. E. and Hellman, L. M. (1938). The production of a gonadotrophic substance (Prolan) by placental cells in tissue culture. *Science (80-.).* **88**, 306-307. doi:10.1126/science.88.2283.306

Giacomini, M. M., Travis, M. A., Kudo, M. and Sheppard, D. (2012). Epithelial cells utilize cortical actin/myosin to activate latent TGF-β through integrin αvβ6-dependent physical force. *Exp. Cell Res.* **318**, 716-722. doi:10.1016/j.yexcr.2012.01.020

Godkin, J. D., Bazer, F. W., Thatcher, W. W. and Roberts, R. M. (1984). Proteins released by cultured Day 15-16 conceptuses prolong luteal maintenance when introduced into the uterine lumen of cyclic ewes. *J. Reprod. Fertil.* **71**, 57-64. doi:10.1530/jrf.0.0710057

Greenstein, J. S., Murray, R. W. and Foley, R. C. (1958). Observations on the morphogenesis and histochemistry of the bovine preattachment placenta between 16 and 33 days of gestation. *Anat. Rec.* **132**, 321-341. doi:10.1002/ar.1091320308

Grosser, O. (1927). *Fruhentwicklung, eihautbildung und placentation des menschen und der saugetiere*. J. F. Bergman: Munchen, Germany.
Hirayama, H., Koyama, K., Sawai, K., Fujii, T., Naito, A., Fukuda, S. and Kageyama, S. (2015). Localization of TGF-β and TGF-β receptor in bovine term placentome and expression differences between spontaneous and induced parturition. *Placenta* **36**, 1239-1245. doi:10.1016/j.placenta.2015.09.003
Hirose, T. (1920). Exogenous stimulation of corpus luteum formation in the rabbit: influence of extracts of human placenta, decidua, fetus, hydatid mole, and corpus luteum on the rabbit gonad. *J. Jpn. Gynecol. Soc.* **16**, 1055.
Huang, D. W., Sherman, B. T. and Lempicki, R. A. (2008). Systematic and integrative analysis of large gene lists using DAVID bioinformatics resources. *Nat. Protoc.* **4**, 44-57. doi:10.1038/nprot.2008.211
Huang, X., Han, X., Uyunbilig, B., Zhang, M., Duo, S., Zuo, Y., Zhao, Y., Yun, T., Tai, D., Wang, C. et al. (2014). Establishment of bovine trophoblast stem-like cells from in vitro - produced blastocyst-stage embryos using two inhibitors. *Stem Cells Dev.* **23**, 1501-1514. doi:10.1089/scd.2013.0329
Imakawa, K., Anthony, R. V., Kazemi, M., Marotti, K. R., Polites, H. G. and Roberts, R. M. (1987). Interferon-like sequence of ovine trophoblast protein secreted by embryonic trophectoderm. *Nature* **330**, 377-379. doi:10.1038/330377a0
Ishizaki, T., Uehata, M., Tamechika, I., Keel, J., Nonomura, K., Maekawa, M. and Narumiya, S. (2000). Pharmacological properties of Y-27632, a specific inhibitor of Rho- associated kinases. *Mol. Pharmacol.* **57**, 976-983.
Jaeger, L. A., Spiegel, A. K., Ing, N. H., Johnson, G. A., Bazer, F. W. and Burghardt, R. C. (2005). Functional effects of transforming growth factor β on adhesive properties of porcine trophectoderm. *Endocrinology* **146**, 3933-3942. doi:10.1210/en.2005-0090
Julian, L. and Olson, M. F. (2014). Rho-associated coiled-coil containing kinases (ROCK), structure, regulation, and functions. *Small GTPases* **5**, e29846. doi:10.4161/sgtp.29846
Kamaraju, A. K. and Roberts, A. B. (2005). Role of Rho/ROCK and p38 MAP kinase pathways in transforming growth factor-β-mediated Smad-dependent growth inhibition of human breast carcinoma cells in vivo. *J. Biol. Chem.* **280**, 1024-1036. doi:10.1074/jbc.M403960200
Kawabata, M., Imamura, T., Inoue, H., Hanai, J.-I., Nishihara, A., Hanyu, A., Takase, M., Ishidou, Y., Udagawa, Y., Oeda, E. et al. (1999). Intracellular signaling of the TGF-β superfamily by Smad proteins. *Ann. N. Y. Acad. Sci.* **886**, 73-82. doi:10.1111/j.1749-6632.1999.tb09402.x
Kawagishi, R., Tahara, M., Sawada, K., Morishige, K., Sakata, M., Tasaka, K. and Murata, Y. (2004). Na+ / H+ exchanger-3 is involved in mouse blastocyst formation. *J. Exp. Zool. A Comp. Exp. Biol.* **301**, 767-775. doi:10.1002/jez.a.90
Kenny, F. N., Drymoussi, Z., Delaine-Smith, R., Kao, A. P., Laly, A. C., Knight, M. M., Philpott, M. P. and Connelly, J. T. (2018). Tissue stiffening promotes keratinocyte proliferation through activation of epidermal growth factor signaling. *J. Cell Sci.* **131**, jcs215780. doi:10.1242/jcs.215780
Kim, D., Pertea, G., Trapnell, C., Pimentel, H., Kelley, R. and Salzberg, S. L. (2013). TopHat2: accurate alignment of transcriptomes in the presence of insertions, deletions and gene fusions. *Genome Biol.* **14**, R36. doi:10.1186/gb-2013-14-4-r36
King, G. J., Atkinson, B. A. and Robertson, H. A. (1980). Development of the bovine placentome from days 20 to 29 of gestation. *J. Reprod. Fertil.* **59**, 95-100. doi:10.1530/jrf.0.0590095
Kingman, H. E. (1948). The placentome of the cow. *Am. J. Vet. Res.* **9**, 125.
Kong, Y. P., Carrion, B., Singh, R. K. and Putnam, A. J. (2013). Matrix identity and tractional forces influence indirect cardiac reprogramming. *Sci. Rep.* **3**, 3474. doi:10.1038/srep03474
Kono, K., Tamashiro, D. A. A. and Alarcon, V. B. (2014). Inhibition of RHO-ROCK signaling enhances ICM and suppresses TE characteristics through activation of Hippo signaling in the mouse blastocyst. *Dev. Biol.* **394**, 142-155. doi:10.1016/j.ydbio.2014.06.023
Krämer, A., Green, J., Pollard, J. and Tugendreich, S. (2014). Causal analysis approaches in Ingenuity Pathway Analysis. *Bioinformatics* **30**, 523-530. doi:10.1093/bioinformatics/btt703
Kümper, S., Mardakheh, F. K., McCarthy, A., Yeo, M., Stamp, G. W., Paul, A., Worboys, J., Sadok, A., Jørgensen, C., Guichard, S. et al. (2016). Rho-associated kinase (ROCK) function is essential for cell cycle progression, senescence and tumorigenesis. *eLife* **5**, e12203. doi:10.7554/eLife.12203
Lane, D. P. (1992). p53, guardian of the genome. *Nature* **358**, 15-16. doi:10.1038/358015a0
Lessey, E. C., Guilluy, C. and Burridge, K. (2012). From mechanical force to RhoA activation. *Biochemistry* **51**, 7420-7432. doi:10.1021/bi300758e
Liu, Z.-G., Hsu, H., Goeddel, D. V. and Karin, M. (1996). Dissection of TNF receptor 1 effector functions: JNK activation is not linked to apoptosis while NF-κB activation prevents cell death. *Cell* **87**, 565-576. doi:10.1016/S0092-8674(00)81375-6
Liu, S., Bou, G., Zhao, J., Guo, S., Guo, J., Weng, X., Yin, Z. and Liu, Z. (2018). Asynchronous CDX2 expression and polarization of porcine trophoblast cells reflects a species-specific trophoderm lineage determination progress model. *Mol. Reprod. Dev.* **85**, 590-598. doi:10.1002/mrd.22994
Livak, K. J. and Schmittgen, T. D. (2001). Analysis of relative gene expression data using real-time quantitative PCR and the $2^{-\Delta\Delta CT}$ method. *Methods* **25**, 402-408. doi:10.1006/meth.2001.1262
Lopata, A. (1996). Molecular aspects of implantation. *Mol. Hum. Reprod.* **2**, 519-525. doi:10.1093/molehr/2.7.519
Ludbrook, S. B., Barry, S. T., Delves, C. J. and Horgan, C. M. T. (2003). The integrin αvβ3 is a receptor for the latency-associated peptides of transforming growth factors β1 and β3. *Biochem. J.* **369**, 311-318. doi:10.1042/bj20020809
McMullan, R., Lax, S., Robertson, V. H., Radford, D. J., Broad, S., Watt, F. M., Rowles, A., Croft, D. R., Olson, M. F. and Hotchin, N. A. (2003). Keratinocyte differentiation is regulated by the Rho and ROCK signaling pathway. *Curr. Biol.* **13**, 2185-2189. doi:10.1016/j.cub.2003.11.050
Melton, A. A., Berry, R. O. and Butler, O. D. (1951). The interval between the time of ovulation and attachment of the bovine embryo. *J. Anim. Sci.* **10**, 993-1005. doi:10.2527/jas1951.104993x
Mi, H., Huang, X., Muruganujan, A., Tang, H., Mills, C., Kang, D. and Thomas, P. D. (2017). PANTHER version 11: expanded annotation data from Gene Ontology and Reactome pathways, and data analysis tool enhancements. *Nucleic Acids Res.* **45**, D183-D189. doi:10.1093/nar/gkw1138
Mi, H., Ebert, D., Muruganujan, A., Mills, C., Albou, L.-P., Mushayamaha, T. and Thomas, P. D. (2021). PANTHER version 16: a revised family classification, tree-based classification tool, enhancer regions and extensive API. *Nucleic Acids Res.* **49**, D394-D403. doi:10.1093/nar/gkaa1106
Morohaku, K., Pelton, S. H., Daugherty, D. J., Butler, W. R., Deng, W. and Selvaraj, V. (2014). Translocator protein/peripheral benzodiazepine receptor is not required for steroid hormone biosynthesis. *Endocrinology* **155**, 89-97. doi:10.1210/en.2013-1556
Mossman, H. W. (1937). Comparative morphogenesis of the metal membranes and accessory uterine structures. *Carnegie Contrib. Embryol.* **26**, 129-246.
Munger, J. S., Huang, X., Kawakatsu, H., Griffiths, M. J. D., Dalton, S. L., Wu, J., Pittet, J.-F., Kaminski, N., Garat, C., Matthay, M. A. et al. (1999). The integrin αvβ6 binds and activates latent TGFβ1: a mechanism for regulating pulmonary inflammation and fibrosis. *Cell* **96**, 319-328. doi:10.1016/S0092-8674(00)80545-0
Munson, L., Wilhite, A., Boltz, V. F. and Wilkinson, J. E. (1996). Transforming growth factor β in bovine placentas. *Biol. Reprod.* **55**, 748-755. doi:10.1095/biolreprod55.4.748
Nakaya, Y., Koshi, K., Nakagawa, S., Hashizume, K. and Miyazawa, T. (2013). Fematrin-1 Is involved in fetomaternal cell-to-cell fusion in bovinae placenta and has contributed to diversity of ruminant placentation. *J. Virol.* **87**, 10563-10572. doi:10.1128/JVI.01398-13
Negrón-Pérez, V. M., Vargas-Franco, D. and Hansen, P. J. (2017a). Role of chemokine (C-C motif) ligand 24 in spatial arrangement of the inner cell mass of the bovine embryo. *Biol. Reprod.* **96**, 948-959. doi:10.1093/biolre/iox037
Negrón-Pérez, V. M., Zhang, Y. and Hansen, P. J. (2017b). Single-cell gene expression of the bovine blastocyst. *Reproduction* **154**, 627-644. doi:10.1530/REP-17-0345
Negrón-Pérez, V. M., Rodrigues, L. T., Mingoti, G. Z. and Hansen, P. J. (2018). Role of ROCK signaling in formation of the trophectoderm of the bovine preimplantation embryo. *Mol. Reprod. Dev.* **85**, 374-375. doi:10.1002/mrd.22976
Okae, H., Toh, H., Sato, T., Hiura, H., Takahashi, S., Shirane, K., Kabayama, Y., Suyama, M., Sasaki, H. and Arima, T. (2018). Derivation of human trophoblast stem cells. *Cell Stem Cell* **22**, 50-63.e6. doi:10.1016/j.stem.2017.11.004
Ozdamar, B., Bose, R., Barrios-Rodiles, M., Wang, H.-R., Zhang, Y. and Wrana, J. L. (2005). Regulation of the polarity protein Par6 by TGFß receptors controls epithelial cell plasticity. *Science (80-.)* **307**, 1603-1609. doi:10.1126/science.1105718
Passegué, E. and Wagner, E. F. (2000). JunB suppresses cell proliferation by transcriptional activation of p16(INK4a) expression. *EMBO J.* **19**, 2969-2979. doi:10.1093/emboj/19.12.2969
Pillai, V. V., Siqueira, L. G., Das, M., Kei, T. G., Tu, L. N., Herren, A. W., Phinney, B. S., Cheong, S. H., Hansen, P. J. and Selvaraj, V. (2019a). Physiological profile of undifferentiated bovine blastocyst-derived trophoblasts. *Biol Open* **8**, bio037937. doi:10.1242/bio.037937
Pillai, V. V., Kei, T. G., Reddy, S. E., Das, M., Abratte, C., Cheong, S. H. and Selvaraj, V. (2019b). Induced pluripotent stem cell generation from bovine somatic cells indicates unmet needs for pluripotency sustenance. *Anim. Sci. J.* **90**, 1149-1160. doi:10.1111/asj.13272
Pillai, V. V., Koganti, P. P., Kei, T. G., Gurung, S., Butler, W. R. and Selvaraj, V. (2021). Efficient induction and sustenance of pluripotent stem cells from bovine somatic cells. *Biol. Open* **10**, bio058756. doi:10.1242/bio.058756
Provenzano, P. P. and Keely, P. J. (2011). Mechanical signaling through the cytoskeleton regulates cell proliferation by coordinated focal adhesion and Rho GTPase signaling. *J. Cell Sci.* **124**, 1195-1205. doi:10.1242/jcs.067009
Rath, N. and Olson, M. F. (2012). Rho-associated kinases in tumorigenesis: re-considering ROCK inhibition for cancer therapy. *EMBO Rep.* **13**, 900-908. doi:10.1038/embor.2012.127
Ridley, A. J. and Hall, A. (1992). The small GTP-binding protein rho regulates the assembly of focal adhesions and actin stress fibers in response to growth factors. *Cell* **70**, 389-399. doi:10.1016/0092-8674(92)90163-7

Roberts, R. M., Leaman, D. W. and Cross, J. C. (1992). Role of interferons in maternal recognition of pregnancy in ruminants. *Proc. Soc. Exp. Biol. Med.* **200**, 7-18. doi:10.3181/00379727-200-43387A
Roberts, R. M., Green, J. A. and Schulz, L. C. (2016). The evolution of the placenta. *Reproduction* **152**, R179-R189. doi:10.1530/REP-16-0325
Robinson, M. D. and Oshlack, A. (2010). A scaling normalization method for differential expression analysis of RNA-seq data. *Genome Biol.* **11**, R25. doi:10.1186/gb-2010-11-3-r25
Saharinen, J., Taipale, J., Monni, O. and Keski-Oja, J. (1998). Identification and characterization of a new latent transforming growth factor-β-binding protein, LTBP-4. *J. Biol. Chem.* **273**, 18459-18469. doi:10.1074/jbc.273.29.18459
Schaumann, E. N., Staddon, M. F., Gardel, M. L. and Banerjee, S. (2018). Force localization modes in dynamic epithelial colonies. *Mol. Biol. Cell* **29**, 2835-2847. doi:10.1091/mbc.E18-05-0336
Schneider, C. A., Rasband, W. S. and Eliceiri, K. W. (2012). NIH Image to ImageJ: 25 years of image analysis. *Nat. Methods* **9**, 671-675. doi:10.1038/nmeth.2089
Sekine, A., Fujiwara, M. and Narumiya, S. (1989). Asparagine residue in the rho gene product is the modification site for botulinum ADP-ribosyltransferase. *J. Biol. Chem.* **264**, 8602-8605. doi:10.1016/S0021-9258(18)81834-8
Shaulian, E. and Karin, M. (2002). AP-1 as a regulator of cell life and death. *Nat. Cell Biol.* **4**, E131-E136. doi:10.1038/ncb0502-e131
Soares, M. J., Varberg, K. M. and Iqbal, K. (2018). Hemochorial placentation: development, function, and adaptations. *Biol. Reprod.* **99**, 196-211. doi:10.1093/biolre/ioy049
Supek, F., Bošnjak, M., Škunca, N. and Šmuc, T. (2011). REVIGO summarizes and visualizes long lists of gene ontology terms. *PLoS ONE* **6**, e21800. doi:10.1371/journal.pone.0021800
Szklarczyk, D., Gable, A. L., Nastou, K. C., Lyon, D., Kirsch, R., Pyysalo, S., Doncheva, N. T., Legeay, M., Fang, T., Bork, P. et al. (2021). The STRING database in 2021: customizable protein-protein networks, and functional characterization of user-uploaded gene/measurement sets. *Nucleic Acids Res.* **49**, D605-D612. doi:10.1093/nar/gkaa1074
Tanaka, S., Kunath, T., Hadjantonakis, A.-K., Nagy, A. and Rossant, J. (1998). Promotion to trophoblast stem cell proliferation by FGF4. *Science (80-.)* **282**, 2072-2075. doi:10.1126/science.282.5396.2072
Tian, Y.-C., Fraser, D., Attisano, L. and Phillips, A. O. (2003). TGF-β1-mediated alterations of renal proximal tubular epithelial cell phenotype. *Am. J. Physiol. Renal Physiol.* **285**, 130-142. doi:10.1152/ajprenal.00408.2002
Viloria-Petit, A. M., David, L., Jia, J. Y., Erdemir, T., Bane, A. L., Pinnaduwage, D., Roncari, L., Narimatsu, M., Bose, R., Moffat, J. et al. (2009). A role for the TGFβ-Par6 polarity pathway in breast cancer progression. *Proc. Natl. Acad. Sci. USA* **106**, 14028-14033. doi:10.1073/pnas.0906796106
Wathes, D. C. and Wooding, F. B. P. (1980). An electron microscopic study of implantation in the cow. *Am. J. Anat.* **159**, 285-306. doi:10.1002/aja.1001590305
Watson, A. J. and Barcroft, L. C. (2001). Regulation of blastocyst formation. *Front. Biosci.* **6**, D708-D730. doi:10.2741/Watson
Wildman, D. E., Chen, C., Erez, O., Grossman, L. I., Goodman, M. and Romero, R. (2006). Evolution of the mammalian placenta revealed by phylogenetic analysis. *Proc. Natl. Acad. Sci. USA* **103**, 3203-3208. doi:10.1073/pnas.0511344103
Wiley, L. M. (1984). Cavitation in the mouse preimplantation embryo: Na/K-ATPase and the origin of nascent blastocoele fluid. *Dev. Biol.* **105**, 330-342. doi:10.1016/0012-1606(84)90290-2
Wimsatt, W. A. (1951). Observations on the morphogenesis, cytochemistry, and significance of the binucleate giant cells of the placenta of ruminants. *Am. J. Anat.* **89**, 233-281. doi:10.1002/aja.1000890204
Wong, S. Y., Ulrich, T. A., Deleyrolle, L. P., MacKay, J. L., Lin, J.-M. G., Martuscello, R. T., Jundi, M. A., Reynolds, B. A. and Kumar, S. (2015). Constitutive activation of myosin-dependent contractility sensitizes glioma tumor-initiating cells to mechanical inputs and reduces tissue invasion. *Cancer Res.* **75**, 1113-1122. doi:10.1158/0008-5472.CAN-13-3426
Wooding, F. B. P. (1992). The synepitheliochorial placenta of ruminants: Binucleate cell fusions and hormone production. *Placenta* **13**, 101-113. doi:10.1016/0143-4004(92)90025-O
Xu, T., Wu, M., Feng, J., Lin, X. and Gu, Z. (2012). RhoA/Rho kinase signaling regulates transforming growth factor-β1-induced chondrogenesis and actin organization of synovium-derived mesenchymal stem cells through interaction with the Smad pathway. *Int. J. Mol. Med.* **30**, 1119-1125. doi:10.3892/ijmm.2012.1107
Yamauchi, S. (1964). Studies on morphogenesis of uterine horn, especially with uterine caruncle in Japanese native cattle. *Jpn J. Zootech. Sci.* **35**, 92-100. doi:10.2508/chikusan.35.tokubetu_92
Ying, Q.-L., Wray, J., Nichols, J., Batlle-Morera, L., Doble, B., Woodgett, J., Cohen, P. and Smith, A. (2008). The ground state of embryonic stem cell self-renewal. *Nature* **453**, 519-523. doi:10.1038/nature06968
Zhang, Y., Wei, Q., Zhao, T., Zhao, P. and Zhang, S. (2019). Extracellular and intercellular force distribution in circularly shaped epithelia. *Extrem. Mech. Lett.* **31**, 100526. doi:10.1016/j.eml.2019.100526
Zondek, B. (1930). Zur methodik der schwangerschaftsreaktion aus dem harne durch nachweis des hypophysenvorder- lappenhormons. *Klin Wchnschr* **9**, 964-966. doi:10.1007/BF01725564
Zondek, B. and Aschheim, S. (1927). Hypophysenvorderlappen und ovarium. *Arch f Gynäk* **130**, 1-45. doi:10.1007/BF01736546